Inorganic Chemistry

Article

pubs.acs.org/IC

A Bispidol Chelator with a Phosphonate Pendant Arm: Synthesis, Cu(II) Complexation, and ^{64}Cu Labeling

Raphaël Gillet,[†] Amandine Roux,[†] Jérémy Brandel,[‡] Sandrine Huclier-Markai,[§,∥] Franck Camerel,[⊥] Olivier Jeannin,[⊥] Aline M. Nonat,*[,†] and Loïc J. Charbonnière*[,†]

[†]Laboratoire d'Ingénierie Moléculaire Appliquée à l'Analyse, Université de Strasbourg, CNRS, IPHC UMR 7178, F-67000 Strasbourg, France

[‡]Laboratoire de Reconnaissance et Procédés de Séparation Moléculaire, Université de Strasbourg, CNRS, IPHC UMR 7178, F-67000 Strasbourg, France

[§]GIP Arronax, 1 rue Aronnax, CS 10112, F-44817 Saint-Herblain, France

[∥]Subatech Laboratory, UMR 6457, Ecole des Mines de Nantes, IN2P3/CNRS, Université de Nantes, 4 rue Alfred Kastler, F-44307 Nantes, France

[⊥]Laboratoire Matière Condensée et Systèmes Électroactifs, Institut des Sciences Chimiques de Rennes, UMR-CNRS 6226, 263 Avenue du Général Leclerc, CS 74205, F-35042 Rennes Cedex, France

Supporting Information

ABSTRACT: Here we present the synthesis and characterization of a new bispidine (3,7-diazabicyclo[3.3.1]nonane) ligand with *N*-methanephosphonate substituents ($\mathbf{L_2}$). Its physicochemical properties in water, as well as those of the corresponding Cu(II) and Zn(II) complexes, have been evaluated by using UV−visible absorption spectroscopy, potentiometry, ^{1}H and ^{31}P NMR, and cyclic voltammetry. Radiolabeling experiments with $^{64}Cu^{II}$ have been carried out, showing excellent radiolabeling properties. Quantitative complexation was achieved within 60 min under stoichiometric conditions, at room temperature and in the nanomolar concentration range. It was also demonstrated that the complexation occurred below pH 2. Properties have been compared to those of the analogue bispidol bearing a *N*-methanecarboxylate substituent ($\mathbf{L_1}$). Although both systems meet the required criteria to be used as new chelator for $^{64/67}$Cu in terms of the kinetics of formation, thermodynamic stability, selectivity for Cu(II), and kinetic inertness regarding redox- or acid-assisted decomplexation processes, substitution of the carboxylic acid function by the phosphonic moiety is responsible for a significant increase in the thermodynamic stability of the Cu(II) complex (+2 log units for pCu) and also leads to an increase in the radiochemical yields with $^{64}Cu^{II}$ which is quantitative for $\mathbf{L_2}$.

INTRODUCTION

Bispidine derivatives are highly preorganized ligands that can accommodate metal ions with cis-octahedral, square-pyramidal, or pentagonal geometries.[1,2] They usually form thermodynamically very stable metal complexes with transition-metal ions which often show high kinetic inertness.[3−5] Modification of the coordinating pendant arms can be used to tune the ligand denticity as well as all electronic, thermodynamic, and kinetic parameters such as the ligand field, the metal selectivity, the stability constants and the redox potentials. Such properties are very appealing for applications in catalysis,[6−12] in molecular magnetism,[13−17] and in nuclear medicine and diagnosis as chelators for $^{64/67}$Cu.[18−21]

This study focuses on the use of two bispidine derivatives ($\mathbf{L_1}$ and $\mathbf{L_2}$, Chart 1) as chelators for radioactive copper for application in immuno-positron emission tomography (PET) (^{64}Cu, $t_{1/2}$ = 12.7 h, β^+, 17.8%, 653 keV, β^-, 38.4%, 579 keV).[22] In this context, bifunctional chelators (BFCs) are needed, providing a strong chelating site for radioactive copper complexation as well as a reactive function for conjugation to a monoclonal antibody (mAb) (or a fragment) of interest. A great deal of progress in antibody technologies as well as site-specific conjugation methods[23,24] has been made in recent years, and it is now within our grasp to find or design engineered mAb fragments for almost any molecular target.[25]

Chart 1. Structures of Acid-Functionalized Ligands ($\mathbf{L_1}$ and $\mathbf{L_2}$) Studied and the Related Bispidone ($\mathbf{L_3}$)

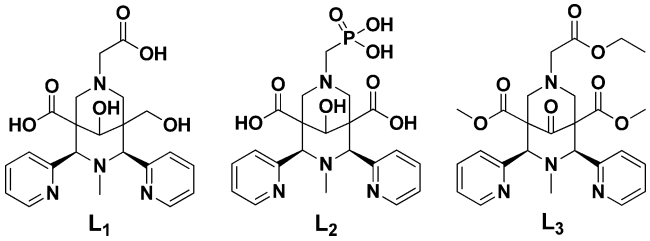

Received: July 7, 2017

DOI: 10.1021/acs.inorgchem.7b01731
Inorg. Chem. XXXX, XXX, XXX−XXX

Chart 2. Structures of Other Ligands Discussed in This Work

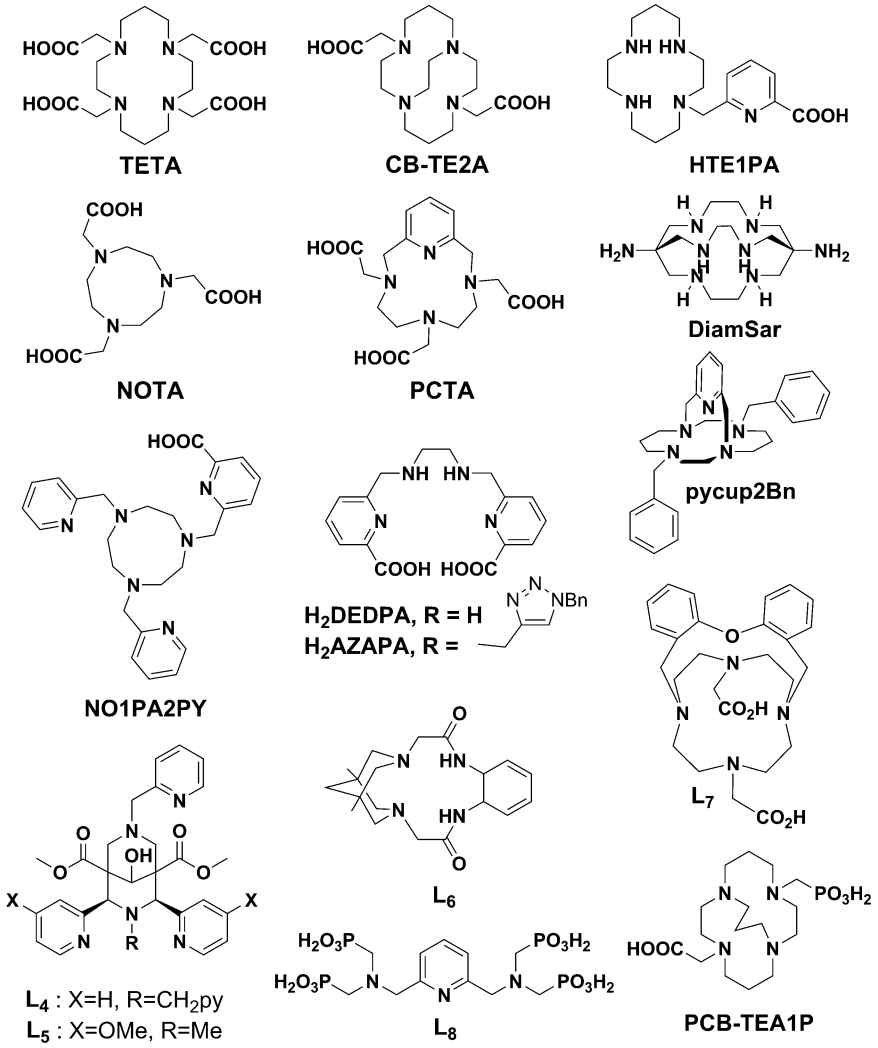

Table 1. Radiolabeling Conditions (at Room Temperature), Half-Life ($t_{1/2}$), pCu, and Reduction Potential (E_{red}) for a Selection of Ligands

	radiolabeling conditions	$t_{1/2}$	pCu[a]	E_{red} (mV vs NHE)
TETA[31,32]	25 °C, 60 min, pH 5−7	3.5 days (5 M HCl, 30 °C)	15.1	−980 (irrev)
CB-TE2A[51]	95 °C, 60 min, pH 6−7	154 h (5 M HCl, 90 °C)		−880 ($E_{1/2}$)
HTE1PA[40,41]	room temp, 15 min, pH 5	32 min (HCl 1 M, 25 °C)	18.64	
		144 min (5 M $HClO_4$, 25 °C)		
CB-TE1PA[94]		96 days (5 M $HClO_4$, 25 °C)	16.6	−620 ($E_{1/2}$)
PCTA[63,35]	25 °C, 5 min, pH 5.5		19.1	
DiamSar[55−57]	25 °C, 5−30 min, pH 5.5	40 h (5 M HCl, 90 °C)		−900 (irrev)
NOTA[30,64,32]	25 °C, 30−60 min, pH 5.5−6.5	<3 min (5 M HCl, 30 °C)	18.4	−700 (irrev)
NO1PA2PY[44]	room temp, 30 min, pH 6−7	204 min (3M, HCl, 90 °C)	17.75	−518
H2DEDPA[53]	25 °C, 5−10 min, pH 5.5	<5 min (6 M HCl, 90 °C)	18.5	−920 (irrev)
H2AZAPA[65]	25 °C, 5−10 min, pH 5.5			
L_1[b21]	room temp, 15 min, pH 2−6	110 d (5 M $HClO_4$, 25 °C)	17.0	−560
L_2[b]	room temp, 5−15 min, pH 3−6.6	>20 months (5 M $HClO_4$, 25 °C)	19.1	−600
L_4[18,4]	room temp, 1 min, pH 6.5		16.28	−303
L_5[19]	room temp, 1 min, pH 5.5			
L_6[20]	50 °C, 60 min, pH 6.5			
PCB-TEA1P[51]	60 °C, 1 h, pH 8	8 days (12 M HCl, 90 °C)		−573
L_7[60,62]			15.5	

[a]Conditions: pCu = $-\log[Cu(II)_{free}]$, [Cu] = 10^{-6} M, [L] = 10^{-5} M, pH 7.4. [b]This work.

DOI: 10.1021/acs.inorgchem.7b01731
Inorg. Chem. XXXX, XXX, XXX−XXX

Scheme 1. Synthesis of Ligand L_2

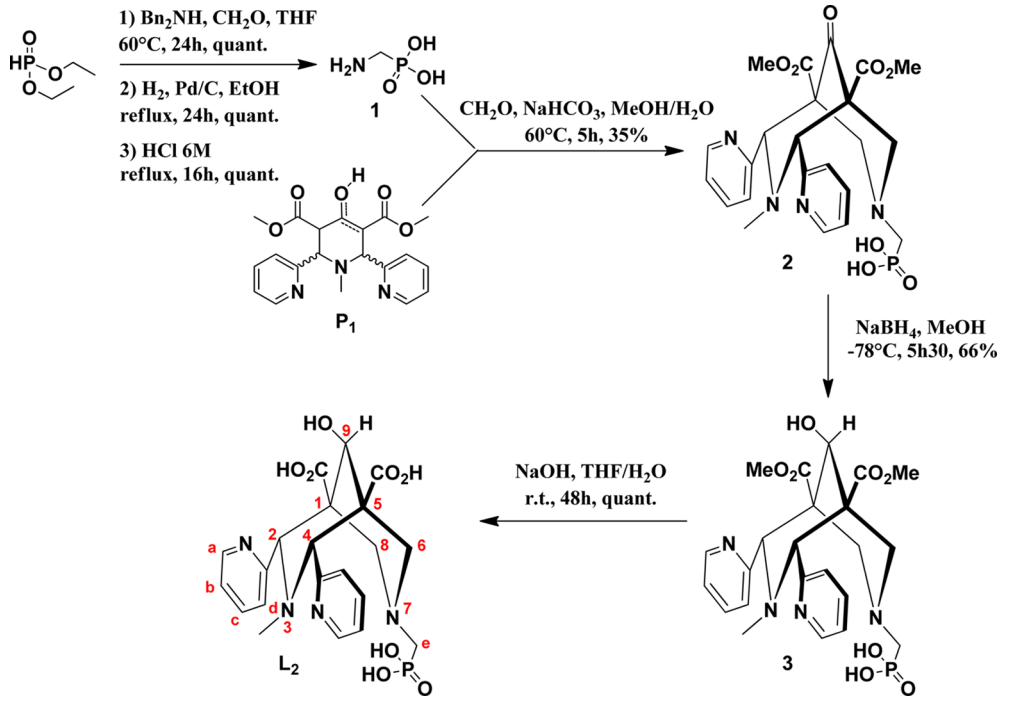

Radiolabeled antibodies have been introduced in clinical use,[26−29] and a large range of BFCs are now available.[30−32] However, only a few chelators fulfill all of the very specific criteria which are required to radiolabel antibody-BFC conjugates under good conditions: i.e., (i) fast radiolabeling (a few minutes to 1 h) at room temperature and around physiological pH; (ii) high in vivo stability and kinetic inertness toward transmetalation, transchelation, and reduction, and (iii) easy access to synthesis and bioconjugation.[33,34]

Three classes of ligands with polyaza donor sets are commonly used: macrocyclic, linear, and macrobicyclic. NOTA[35,36] and TETA[37−39] and their derivatives are easily accessible but often suffer from low kinetic inertness. Variations of the substituent are being explored in order to improve the in vivo stability of the Cu complexes (see HTE1PA[40−43] and NO1PA2PY[44] and its derivatives,[45] Chart 2 and Table 1). Very stable and inert cyclen-based cross-bridged systems (such as PycupBn[46] and CB-TE2A,[47] Chart 2) and macrobicycles such as $\mathbf{L}_7$[48] are being developed, but their slow kinetics of complexation is hampering their use for the labeling of antibodies. Faster complexation is observed with *N*-phosphonic acid analogues, although heating is still necessary for the moment.[49−52] New linear systems such as H_2DEDPA and H2AZAPA[53,54] as well as other types of macrocyclic ligands and cages (DiamSar[55−57] and its derivatives) offer good radiolabeling conditions at room temperature (Chart 2) and, for some of them, a high degree of kinetic inertness. Bispidine derivatives ($\mathbf{L}_4$ and $\mathbf{L}_5$, Chart 2) also form particularly stable Cu(II) complexes in vitro and in vivo. $\mathbf{L}_4$ and $\mathbf{L}_5$ could be radiolabeled with >95% radiolabeling yields within 1 min at room temperature.[4,18] Nonoptimized specific activities of less than 0.1 GBq/μmol were used for $\mathbf{L}_4$[18] and $\mathbf{L}_5$,[19] and a specific activity of 26 GBq/μmol was obtained for $\mathbf{L}_6$ after 90 min at 50 °C.[20] Preliminary in vivo studies in mice and rats for $\mathbf{L}_4$ and $\mathbf{L}_6$ indicated rapid blood and tissue clearance as well as the absence of demetalation. However, changes were observed over time in the radio-HPLC chromatogram of $\mathbf{L}_4$, which were attributed to partial or total hydrolysis of the ester functions by the esterase in rat plasma.[18] Dioxotetraaza macrocycles ($\mathbf{L}_6$, Chart 2) are also very stable, although efficient labeling was observed only after heating the samples at 50 °C.[20]

Our previous studies on the methylene carboxylate substituted bispidine $\mathbf{L}_1$ have shown that this ligand is another good candidate for PET applications.[21] Fast complexation occurs even at low pH values (pH 1), with a high binding constant for Cu(II) versus competing metals (Co(II), Ni(II), Zn(II)), and the complex is characterized by a strong stability in acidic medium ($t_{1/2}$ = 110 days at 25 °C, 5 M $HClO_4$) and upon reduction ($E_{1/2}$ = −430 mV vs NHE). Radiolabeling with $^{64}CuCl_2$ is fast (<5 min) and easily performed at room temperature and at micromolar concentrations of $\mathbf{L}_1$ in water ($4 \leq pH \leq 6$).[58] Under these conditions, ≥90% radiolabeling yields were obtained. Moreover, the risk of enzymatic degradation is suppressed since the ester functions have been hydrolyzed prior to complexation. In this study, we report the synthesis and physicochemical evaluation and the radiolabeling studies of the new methane phosphonate analogue $\mathbf{L}_2$ in water. Substitution of the acetic acid pendant arm by a methanephosphonic acid moiety was expected to improve the ligand selectivity for Cu(II) and to increase the thermodynamic and kinetic stability of the complex. This expectation is corroborated by literature data on phosphonate pendant-armed tetraazamacrocyclic chelators such as PCB-TEA1P[51,59] as well as on the podal pyridine derivatives developed in our group, $\mathbf{L}_8$ (Chart 2).[60−62]

EXPERIMENTAL SECTION

General Methods. Solvents and starting materials were purchased from Aldrich, Acros, and Alfa Aesar and used without further purification. IR spectra were recorded on a PerkinElmer Spectrum One spectrophotometer as solid samples, and only the most significant absorption bands are given in cm^{-1}. Elemental analyses and mass spectrometry analysis were carried out by the Service Commun

DOI: 10.1021/acs.inorgchem.7b01731
Inorg. Chem. XXXX, XXX, XXX−XXX

d'Analyses of the University of Strasbourg. ^{1}H and ^{13}C NMR spectra and 2D COSY, NOESY, HSQC, and HMBC experiments were recorded on Bruker Avance 300 and Avance 400 spectrometers operating at 300 and 400 MHz, respectively. Chemical shifts are reported in ppm, relative to residual protonated solvent as internal reference.[66] The pH values given are corrected for the deuterium isotopic effects.[67] Elemental analysis and monoisotopic masses were calculated with the Chemcalc software.[68]

X-ray Crystallography. Crystals of the intermediate **2** (Scheme 1) and $\mathbf{L_2}$ ligand suitable for X-ray diffraction were obtained by slow evaporation of methanol solutions. The crystals were placed in oil, and a single crystal was selected, mounted on a nylon loop, and placed in a low-temperature N_2 stream. X-ray diffraction data collection was carried out on a Bruker APEX II Kappa-CCD diffractometer equipped with an Oxford Cryosystem liquid N_2 device, using Mo Kα radiation (λ = 0.71073 Å) at 150(2) K (Centre de diffractométrie X, Université de Rennes 1, France). The Bruker SMART program was used to refine the values of the cell parameters. Data reduction and correction for absorption (SADABS) were carried out using the Bruker SAINT programs. The structures were solved by direct methods using the SIR97 program[69] and then refined with full-matrix least-squares methods based on F^2 (SHELX-97)[70] with the aid of the WINGX program.[71] All non-hydrogen atoms were refined with anisotropic atomic displacement parameters.

For **2**, all H atoms were included in their calculated positions, whereas, for $\mathbf{L_2}$, H atoms carried by heteroatoms were refined with isotropic atomic displacement parameters. Crystallographic data for structural analysis of **2** and ligand $\mathbf{L_2}$ have been deposited with the Cambridge Crystallographic Data Centre under CCDC nos. 1530206 and 1530205, respectively. Copies of this information may be obtained free of charge from the Web site (www.ccdc.cam.ac.uk).

Synthesis of the Ligands. Piperidinone dimethyl-1-methyl-4-oxo-2,6-bis(pyridin-2-yl)piperidine-3,5-dicarboxylate ($\mathbf{P_1}$) was synthesized according to a previously reported procedure.[72]

(Aminomethyl)phosphonic Acid ***1***. **1** was obtained in three steps from diethyl phosphate by the Kabachnik–Fields reaction, according to an adaptation of the procedure used in ref 73.

(i) To a solution of diethyl phosphite (3.27 mL, 94%, 20.7 mmol, 1.2 equiv) in THF (9 mL) were successively added dibenzylamine (3.39 mL, 98%, 17.27 mmol, 1 equiv) and formaldehyde (3.06 mL, 37% in water, 34.5 mmol, 2 equiv). The mixture was heated at 60 °C with stirring for 24 h, and the reaction was monitored by TLC. After completion of the reaction, the mixture was taken to dryness under vacuum and the as-obtained yellow oil was dissolved in cyclohexane (60 mL) and washed with water (3 × 15 mL). Diethyl ((dibenzylamino)methyl)phosphonate was obtained as a colorless oil after evaporation of the cyclohexane under reduced pressure (6 g, quantitative). ^{1}H NMR (400 MHz, $CDCl_3$): δ 1.19 (t, J = 7.1 Hz, 6H, CH_2CH_3), 2.77 (d, J = 10.5 Hz, 2H, NCH_2P), 3.67 (s, 4H, $NCH_2\Phi$), 3.95 (qd, J_1 = 7.1 Hz, J_2 = 7.5 Hz, 4H, CH_2CH_3), 7.11–7.28 (m, 10H, Φ). ^{31}P NMR (162 MHz, $CDCl_3$): δ 25.7.

(ii) Palladium over charcoal (10%, 600 mg) was added to a solution of diethyl ((dibenzylamino)methyl)phosphonate (6 g, 17.27 mmol) in EtOH (300 mL), and the mixture was refluxed under a flow of hydrogen for 24 h. The crude mixture was filtered on a sintered-glass filter funnel filled with Celite, and the solvent was removed under vacuum to yield diethyl (aminomethyl)phosphonate (4.8 g, quantitative). ^{1}H NMR (400 MHz, $CDCl_3$): δ 1.25 (t, J = 6.7 Hz, 6H, CH_2CH_3), 1.97 (s, 2H, NH_2), 2.94 (d, J = 10.2 Hz, 2H, NCH_2P), 4.05 (m, 4H, CH_2CH_3). ^{31}P NMR (162 MHz, $CDCl_3$): δ 27.35 ppm (qd, J_1 = 8.5 Hz, J_2 = 9.2 Hz).

(iii) Diethyl (aminomethyl)phosphonate (4.81 g, 28.8 mmol) was dissolved in 6 M hydrochloric acid (300 mL), and the mixture was refluxed for 16 h with stirring. After evaporation to dryness under reduced pressure, (aminomethyl)phosphonic acid **1** was obtained as a white powder (4.25 g, quantitative). ^{1}H NMR (400 MHz, $CDCl_3$): δ 3.00 (d, J = 13.0 Hz, 2H). ^{31}P NMR (162 MHz, $CDCl_3$): δ 12.18 ppm.

Bispidone ***2***. (Aminomethyl)phosphonic acid **1** (126 mg, 1.13 mmol, 1.1 equiv) was dissolved in a H_2O/MeOH (3/7) mixture (11 mL) and stirred at room temperature in the presence of sodium hydrogenocarbonate (143 mg, 1.7 mmol, 1.7 equiv). Piperidone $\mathbf{P_1}$ (396 mg, 1.0 mmol, 1 equiv) in 8 mL of MeOH was then added, as well as formaldehyde (93.0 mg, 3.1 mmol, 3 equiv, 0.23 mL, 37% solution in H_2O). The reaction mixture was heated to 60 °C for 5 h, the reaction being monitored by TLC on (eluent DCM/MeOH 9/1, R_f = 0.26). After completion of the reaction, the solvent was evaporated under reduced pressure and the crude product was suspended in EtOH (10 mL). Bispidone **2** was isolated by centrifugation as a white powder (187 mg, 35%). ^{1}H NMR (400 MHz, CD_3OD): δ 1.87 (s, 3H, H3), 2.53 (d, J = 13.0 Hz, 2H, He), 3.15 (AB system, δ_A = 2.66, δ_B = 3.64, J_{AB} = 12.3 Hz, 4H, H6/H8), 3.72 (s, 6H, OCH_3), 4.68 (s, 2H, H2/H4), 7.35 (m, 2H, Hd), 7.42 (ddd, J_1 = 7.7 Hz, J_2 = 4.9 Hz, J_3 = 0.9 Hz, 2H, Hb), 7.84 (td, J_1 = 7.8 Hz, J_2 = 1.5 Hz, 2H, Hc), 8.83 (dd, 2H, Ha). ^{31}P NMR (162 MHz, CD_3OD): δ 15.29 ppm. ^{13}C NMR (100 MHz, CD_3OD): δ 41.9 (CH_3), 51.7 (2C, OCH_3), 57.2 (d, Ce), 60.9 (2C, C6), 63.0 (2C, C1), 72.4 (2C, C2), 123.8 (2C, Cb), 124.7 (2C, Cd), 137.6 (2C, *Cc*), 150.6 (2C, Ca), 156.3 (2C, Cpy), 167.5 (2C, CO_2Me), 202.3 (C9). Electrospray ionization (ESI)/MS^+ (CH_3OH): m/z 519.17 ($[M + H]^+$, 100%). Anal. Calcd for $C_{23}H_{26}N_4O_8PNa{\cdot}0.5H_2O$: C, 50.28; H, 4.95; N, 10.20. Found: C, 50.39; H, 4.75; N, 10.27.

Bispidol ***3***. Compound **2** (1.2 g, 2.3 mmol, 1 equiv) was dissolved in 80 mL of anhydrous MeOH by heating and using ultrasound. The solution was then cooled to −78 °C, and sodium borohydride (107 mg, 2.8 mmol, 1.5 equiv) was gradually added. The reaction was monitored by TLC on C18 (eluent H_2O/ACN 7/3, R_f = 0.28). After 5 h 30 min, the reaction was quenched at −78 °C by the addition of a saturated NH_4Cl aqueous solution (5 mL). The solvent was evaporated under vacuum, and the crude product was purified by FPLC on a C18 reverse phase column (eluent system H_2O/ACN 0.1% TFA), giving the bispidol **3** (0.79 g, 66%). ^{1}H NMR (400 MHz, CD_3OD): δ 1.74 (s, 3H, H3), 3.35 (d, J = 11 Hz, 2H, He), 3.62 (s, 6H, OCH_3), 4.0 (AB system, δ_A 3.76, H6/8ax, δ_B 4.23, H6/8eq, J = 12.7 Hz, 4H), 4.55 (s, 1H, H9), 4.98 (s, 2H, H2/H4), 7.43 (dd, J_1 = 7.0 Hz, J_2 = 5.2 Hz, 2H, Hb), 7.65 (d, J = 7.6 Hz, 2H, Hd), 7.87 (td, J_t = 7.7 Hz, J_d = 1.6 Hz, 2H, Hc), 8.74 (d, J = 4.1 Hz, 2H, Ha). ^{31}P NMR (162 MHz, CD_3OD): δ 8.24 ppm. ^{13}C NMR (100 MHz, CD_3OD): δ 40.7 (CH_3), 51.2 (2C, C1), 51.8 (2C, OCH_3), 53.2 (d, J = 133.9 Hz, Ce), 55.8 (2C, C6), 66.2 (2C, C2), 71.9 (C9), 123.9 (2C, Cb), 127.6 (2C, Cd), 137.4 (2C, *Cc*), 149.3 (2C, Ca), 155.5 (2C, Cpy), 168.7 (2C, CO_2Me). Electrospray ionization (ESI)/MS^+ (CH_3OH): m/z 521.18 ($[M + H]^+$, 100%). Anal. Calcd for $C_{23}H_{29}N_4O_8P{\cdot}0.5H_2O$: C, 52.17; H, 5.71; N, 10.58. Found: C, 51.94; H, 5.56; N, 10.41.

Ligand $\mathbf{L_2}$. Compound **3** (514 mg, 1 mmol, 1 equiv) was dissolved in a THF/H_2O (1/1) mixture (30 mL), and a solution of sodium hydroxide (200 mg, 5 mmol, 5 equiv) in water (5 mL) was added. The mixture was stirred at room temperature, and the reaction was monitored by TLC (eluent system H_2O/ACN 8/2, 0.1% TFA, R_f = 0.65). After completion of the reaction, the mixture was evaporated to dryness, redissolved in 1 M hydrochloric acid, and purified by flash chromatography with a C18 reverse phase column (eluent system H_2O/ACN 0.1% TFA), to give ligand $\mathbf{L_2}{\cdot}NaCl{\cdot}4H_2O$ (621 mg, quantitative). ^{1}H NMR (300 MHz, CD_3OD): δ 1.78 (s, 3H, NCH_3), 2.34 (d, J = 12.2 Hz, 2H, He), 2.67 (AB system, δ_A 2.09, H6/8ax, δ_B 3.24, H6/8eq, J_{AB} = 12.4 Hz, 4H), 3.88 (s, 1H, H9), 4.61 (s, 2H, H2/H4), 7.24 (m, 2H, Hb), 7.47 (d, J = 7.6 Hz, 2H, Hd), 7.65 (t, J = 7.3 Hz, Hc), 8.76 (d, J = 3.7 Hz, 2H, Ha). ^{31}P NMR (162 MHz, CD_3OD): δ 16.28 ppm (t, J = 12.0 Hz). ^{13}C NMR (100 MHz, CD_3OD): δ 42.9 (CH_3), 51.7 (2C, C1), 59.2 (2C, C6), 60.5 (d, J = 145.7 Hz, C9), 68.3 (2C, C2), 74.8 (C9), 122.0 (Cb), 125.7 (Cd), 136.1 (Cc), 149.5 (Ca), 160.62 (2C, Cpy), 178.34 (2C, CO_2H). Electrospray ionization (ESI)/MS^+ (CH_3OH): m/z 493.15 $[M + H]^+$, 100%). Anal. Calcd for $C_{21}H_{25}N_4O_8P{\cdot}NaCl{\cdot}4H_2O$: C, 40.49; H, 5.34; N, 8.99. Found: C, 40.32; H, 5.03; N, 8.92.

Physicochemical Studies. *Materials.* Distilled water was purified by passing through a mixed bed of ion exchanger (Bioblock Scientific R3–83002, M3-83006) and activated carbon (Bioblock Scientific ORC-83005). All of the stock solutions were prepared by weighing solid products using an AG 245 Mettler Toledo analytical balance (precision 0.01 mg). Metal cation solutions were prepared from their

DOI: 10.1021/acs.inorgchem.7b01731
Inorg. Chem. XXXX, XXX, XXX–XXX

perchlorate salts ($Cu(ClO_4)_2 \cdot 6H_2O$, 98%, Fluka; $Zn(ClO_4)_2 \cdot 6H_2O$, 98.9%, Alfa Aesar), and their concentrations were determined by colorimetric titrations with EDTA (10^{-2} M, Merck, Titriplex III) according to standard procedures.[74] Sodium hydroxide (NaOH) and hydrochloric acid (HCl) were used to adjust pH during titrations. The ionic strength of all the solutions was fixed to 0.1 M with potassium chloride (KCl, Fluka, 99.0%). All of the experiments described were repeated at least three times.

Caution! Perchlorate salts combined with organic ligands are potentially explosive and should be handled in small quantities and with adequate precautions.[75]

Potentiometry. The protonated species of $\mathbf{L_2}$ and the stability constants of $\mathbf{L_2}$ complexes with Cu(II) and Zn(II) complexes were characterized and quantified by potentiometric titrations in water. All of the solutions used in the potentiometric experiments were prepared from boiled and degassed water. Titrations were performed using an automated titrating system (DMS 716 Titrino, Metrohm) with a combined glass electrode (Metrohm, 6.0234.100, Long Life) filled with NaCl 0.1 M. The electrode was calibrated as a hydrogen concentration probe by titrating known amounts of hydrochloric acid with CO_3^{2-}-free potassium hydroxide solutions. The GLEE program[76,77] was used for the glass electrode calibration.

In a typical experiment, an aliquot of 10 mL of $\mathbf{L_2}$ (2.10^{-3} M) or M/$\mathbf{L_2}$ (M = Cu(II), Zn(II), [M]/[L] ≈ 1) was introduced into a thermostated jacketed cell (25.0(2) °C, Metrohm) and kept under argon during the titrations. The solutions were acidified with a known volume of HCl, and the titrations were then carried out by addition of known volumes of potassium hydroxide solution over the pH range 2−12. The potentiometric data of $\mathbf{L_2}$ and its metal complexes were refined with the Hyperquad 2008 program,[78] which uses nonlinear least-squares methods, taking into account the formation of metal hydroxide species. The titration of each system was repeated at least in duplicate, and the sets of data for each system were treated independently and then merged together and treated simultaneously to give the final stability constants. The distribution curves as a function of pH of the protonated species of $\mathbf{L_2}$ and of $\mathbf{L_2}$ metal complexes were calculated using the Hyss2009 program.[79]

Spectrophotometry. The protonation constants of $\mathbf{L_2}$ and the stability constants of M/$\mathbf{L_2}$ (M = Cu(II), Zn(II), [M]/[L] ≈ 1, [L] ≈ 5×10^{-5} M) were also determined by UV−visible spectrophotometric titration versus pH. Since complexation started in very acidic medium, the titrations were carried out in two different ways. Between pH −0.6 and pH 2, batch solutions were prepared. Each sample was prepared separately by mixing a known amount of $\mathbf{L_2}$ stock solution, a known amount of standardized $HClO_4$ to adjust the pH (pH = −log [H^+]), and a known amount of Cu(II) stock solution in the case of the study of the complexes ([Cu(II)]/[L] = 1). An absorption spectrum of each sample was recorded in a 1 cm quartz Suprasil spectrophotometric cell using a Varian (Cary 3) UV−visible spectrophotometer. Between pH 2 and 12.5, direct titrations were carried out. Typically, an aliquot of 10 mL of L solution was introduced into a thermostated jacketed titration vessel (25.0(2) °C) with 1 equiv of metal (M) in the case of M/L titrations. A known volume of hydrochloric acid solution was added to adjust the pH to around 2, and the titrations were carried out by addition of known volumes of potassium hydroxide solution. After each addition, the pH was allowed to equilibrate, an aliquot was transferred to a 1 cm quartz Suprasil spectrophotometric cell, a spectrum was recorded using a Varian (Cary 3) spectrophotometer, the aliquot was transferred back to the titration vessel, and a new addition was made. The free hydrogen ion concentrations were measured with a Mettler Toledo U402-S7/120 (pH 0−14) combined glass electrode. Potential differences were given by a Tacussel LPH430T millivoltmeter. Standardization of the millivoltmeter and verification of the linearity of the electrode were performed with three commercial buffer solutions (pH 4.01, 7.01, and 10.01, 25 °C). The software Hypspec V1.1.33 was used to determine the coordination model and calculate the stability constants (log β) of the formed species.[71,80]

Acid Decomplexation Studies. Acid-decomplexation studies were performed under pseudo-first-order conditions on two solutions of $Cu\mathbf{L_2}$ complex in 5 M $HClO_4$ at 25 °C. Changes in the absorption spectra with time over a period of 20 months were monitored using a PerkinElmer Lambda 950 spectrophotometer. A 1.98×10^{-4} mmol portion of $Cu^{II}\mathbf{L_2}$ complex was used to monitor the $\pi-\pi^*$ transition at 262 nm and 8.78×10^{-3} mmol to follow the d−d transition at 680 nm.

Cyclic Voltammetry. Cyclic voltammetry (CV) was carried out on the $Cu\mathbf{L_2}$ complex at room temperature with a PC interfaced Radiometer Analytical MDE150/PST50 instrument. The CV experiments were performed using a glassy-carbon working electrode (0.071 cm^2, BASi). The electrode surface was polished routinely with 0.05 μm alumina−water slurry on a felt surface immediately before use. The counter electrode was a Pt coil, and the reference electrode was a Ag/AgCl electrode. The $Cu\mathbf{L_2}$ complex was measured in Ar-degassed water with ionic strength fixed at 0.1 M with $NaClO_4$, and the pHs of the solutions were adjusted with NaOH and $HClO_4$ solutions. Seven different values of pH (pH 2.36, 4.04, 5.70, 7.2, 8.55, 10.23, 11.62) and different scan rates (50−300 mV/s) were considered.

Radiolabeling. $^{64}CuCl_2$ in 0.1 M hydrochloric acid was obtained from the ARRONAX cyclotron (Saint-Herblain, France). Production and purification procedures have already been described.[81] Radiochemical purity was determined by γ spectroscopy, and chemical purity was measured by ICP-AES. Water (18.2 MΩ cm) for aqueous solutions was obtained from a Milli-Q gradient system (Millipore). Radiolabeling of ligand $\mathbf{L_2}$ with ^{64}Cu was performed, following the same procedure as that previously described for ligand $\mathbf{L_1}$.[58] Postprocessed ^{64}Cu eluate diluted in 0.25 M ammonium acetate buffer (pH 5.3) was mixed at room temperature with a ligand stock solution ($[\mathbf{L_2}]_{stock} = 4.1 \times 10^{-4}$ M). Four radionuclide batches were used for radiolabeling purposes. Each batch was characterized with regard to its specific activity (SA(^{64}Cu) per nmol of Cu) and the content of cold metallic impurities. Briefly, the characteristics of each batch (1−4) are given: batch 1, 13.13 MBq/mL, $[Cu^{2+}] = 4.02 \times 10^{-7}$ M, $[M] = 2.48 \times 10^{-5}$ M, SA(^{64}Cu) = 34.8 MBq/nmol; batch 2, 55.71 MBq/mL, $[Cu^{2+}] = 2.19 \times 10^{-6}$ M, $[M] = 8.93 \times 10^{-6}$ M, SA(^{64}Cu) = 25.3 MBq/nmol; batch 3, 38.94 MBq/mL, $[Cu^{2+}] = 1.53 \times 10^{-6}$ M, $[M] = 8.94 \times 10^{-6}$ M, SA(^{64}Cu) = 25.3 MBq/nmol; batch 4, 9.74 MBq/mL, $[Cu^{2+}] = 3.8 \times 10^{-7}$ M, $[M] = 8.94 \times 10^{-6}$ M, SA(^{64}Cu) = 25.3 MBq/nmol. Several parameters were scrutinized in repeated experiments such as the pH of the reaction mixtures, the time, and the ligand/metal molar ratio (where [metal] corresponds to the total concentration in metal salts, including nonradioactive contaminants from the source such as Co(II), Cu(II), Fe(II/III), Ni(II), and Zn(II)). In typical experiments, 500 μL batch solutions were prepared separately by mixing a known amount of ^{64}Cu stock solution (5−40 μL, 0.5 MBq), a known volume of ligand stock solution, and a known amount of $AcONH_4$ buffer, the pH being previously adjusted to the desired value (2 ≤ pH ≤ 7). The influence of temperature and incubation time on the reaction yield was also investigated on $\mathbf{L_2}$ for an L/M ratio of 0.25 by heating the samples for 1 h at 80 °C; the pH was measured before and after the heating.

Radiolabeling was followed by spotting the reaction mixture onto a TLC Flex Plate (silica gel 60A, lF-254, 200 μm, Merck) followed by elution with concentrated aqueous NH_3/MeOH/H_2O 1/2/1 (v/v/v). Quantitative distribution of radioactivity on TLC plates was measured using an electronic autoradiography system (Cyclone, PerkinElmer). Under these conditions the ^{64}Cu complexes ($R_f = 0.9$) and the free ^{64}Cu ($R_f < 0.1$) are well separated. All yields are given with the experimental uncertainties of the cyclone device of ±5%.

RESULTS AND DISCUSSION

Synthesis of Ligand $\mathbf{L_2}$. Ligand $\mathbf{L_2}$ was obtained in three steps from (aminomethyl)phosphonic acid **1** and the piperidinone precursor $\mathbf{P_1}$ following a synthetic strategy similar to that previously reported for the glycinate derivative $\mathbf{L_1}$ (Scheme 1).[21] **1** was quantitatively obtained by a Kabachnik−Fields reaction of diethyl phosphite, methanal, and dibenzylamine. Hydrogenolysis of the benzyl protecting groups followed by acid hydrolysis of the diethyl ester moieties was

DOI: 10.1021/acs.inorgchem.7b01731
Inorg. Chem. XXXX, XXX, XXX−XXX

performed by using standard conditions. Bispidone **2** was obtained in 35% yield by a double Mannich reaction using $\mathbf{P_1}$, **1**, and methanal in the presence of $NaHCO_3$. By this method, pure bispidone **2** could be obtained by precipitation from ethanol. It can be noted that previous attempts using diethyl(aminomethyl)phosphonate instead of the phosphonic acid led to a mixture of products which was difficult to purify by crystallizations or column chromatography. Selective reduction of the central ketone of **2** was achieved in good yield by addition of $NaBH_4$ in cold methanol (−78 °C). A single epimer, with H_9 pointing toward N_7, was isolated after purification by reverse phase flash chromatography (FPLC) on a C18 column, as evidenced by $^1H-^1H$ NOESY experiments. Interestingly, the same regioselectivity was previously observed with acetate-substituted bispidol,[21] suggesting a facial regioselectivity, which is probably due to the stabilization of the borohydride intermediate due to formation of hydrogen bonds with the carbonyl and acid protons of the phosphonic or carboxylic acid on N_7 (see numbering in Scheme 1). Saponification of the methyl ester substituents was achieved at room temperature in the presence of sodium hydroxide, and the pure ligand could be isolated by reverse phase FPLC (see Figures S1−S13 in the Supporting Information for the NMR spectra of **2**, **3** and $\mathbf{L_2}$).

Structural Characterization of 2 and $\mathbf{L_2}$. Single crystals of **2** (as the sodium salt **2Na**) and $\mathbf{L_2}$ were obtained by slow evaporation of methanol solutions at room temperature. The crystal structure refinement confirms the chemical structures of **2** and ligand $\mathbf{L_2}$. The corresponding ORTEP view of the asymmetric unit is shown in Figures 1 and 2, respectively, and corresponding crystallographic data are presented in Tables 2 and 3.

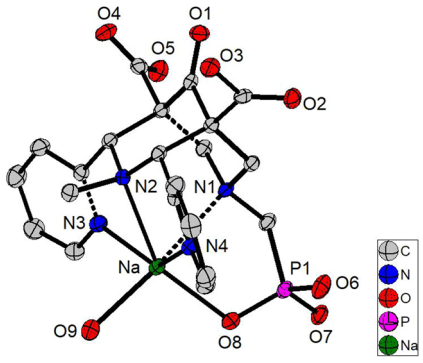

Figure 1. ORTEP drawing of **2Na** with the main atomic numbering. Thermal ellipsoids are drawn at the 50% probability level. All H atoms are omitted for the sake of clarity.

The intermediate **2** was isolated as a sodium salt, and the structure (Figure 1) confirms the chair−chair conformation of the bispidone, as observed by ^1H NMR studies (Figure S1 in the Supporting Information). This intermediate was crystallized in the triclinic space group $P\bar{1}$ with one sodium complex and one methanol molecule in general positions. The Na(I) ion is hexacoordinated by ligand **2** and one methanol molecule with a distorted-octahedral coordination geometry (Table 2), which is, as expected from the strong rigidity of the ligand backbone, very similar to other hexacoordinated structures with Li(I)[82] or transition-metal ions such as Cr(III), Mg(II), Fe(II), Co(II), Cu(I/II), and Zn(II).[5] In the case of $\mathbf{L_2}$, the asymmetric unit contains one complete $\mathbf{L_2}$ ligand and two methanol molecules

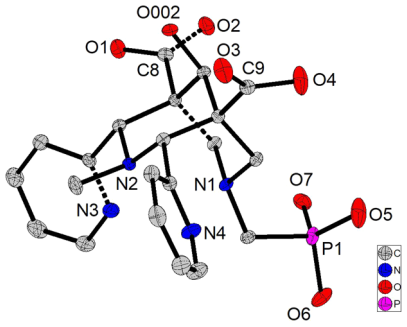

Figure 2. ORTEP drawing of ligand $\mathbf{L_2}$ with the main atomic numbering. Thermal ellipsoids are drawn at the 50% probability level. All H atoms are omitted for the sake of clarity.

in general positions (Figure 2). The ligand crystallizes in a partially protonated form in the monoclinic space group $P2_1/n$ (Table 2) and is characterized by the presence of four acidic protons: one on the carboxylic acid (C9−O4H = 1.3150(16) Å and C9 = O3 = 1.2035(16) Å), two on the phosphonic acid (P1═O5 = 1.4779(0) Å, P1═O6H = 1.5598(10) Å, and P1═O7H = 1.5616(10) Å), and one localized on the tertiary amine R_3NH^+ (N_2-H_2 = 0.894(17) Å). The carbon−oxygen distances on the remaining carboxylate are almost identical (C_8-O_1 = 1.2534(15) Å and C_8-O_2 1.2642(15) Å), and the oxygen atoms O_1 and O_2 are involved in hydrogen bonds with a bidentate phosphonate of a neighboring molecule. Furthermore, the ammonium proton H_2 is stabilized inside the cavity by strong hydrogen bonds with the nitrogen atoms N_1 (d_{H-N1} = 2.1142(105) Å), N_3 (d_{H-N3} = 2.3543(78) Å), and N_4 (d_{H-N4} = 2.5267(86) Å). Deeper analysis of the Fourier transform of the structure factors did not reveal any residual electron density around nitrogen atom N1, meaning that, in the solid state, the proton is exclusively well localized on the nitrogen atom N2. This protonation scheme is typical of a Proton Sponge behavior, which was confirmed by physicochemical titrations (see below). As a consequence, ligand $\mathbf{L_2}$ is highly preorganized for metal complexation with (i) a chair−chair conformation of the bispidine skeleton, (ii) a cis-symmetrical configuration of the pyridine rings, and (iii) the lone pairs of N1 and N2 pointing toward the inside of the cavity. In addition, the N1···N2 = 2.6935(13) and N3···N4 = 4.6913(16) Å distances are significantly shorter than those for analogous bispidone in their deprotonated form (N1···N2 = 2.888(2) and N3···N4 = 7.186(2) Å for $\mathbf{L_3}$)[72] and very close to the distances measured for **2Na** and for another recent example of protonated structure with Hbispa ligands (N1···N2 = 2.684(2) and N3···N4 = 4.922(3) Å for Hbispa1a).[83] This contraction of the cavity is also likely attributed to the presence of the protonated ammonium center, which more strongly attracts the electron-rich surrounding nitrogen atoms. Moreover, the structure is stabilized by a network of strong hydrogen bonds between the phosphonic acids and the acetate moiety of a neighboring molecule (O1−O6 = 2.5404(13) Å, O1−H6A−O6 = 169.8(2)°, O2−O7 = 2.5632(13) Å, O2−H7A−O7 = 177.8(2)° Å), which stabilizes this particular protonation state. Finally, each ligand forms moderate H bonds (O2−O8 = 2.8016(18) Å, O2−H8−O8 = 157.2(1)°, O9−O002 = 2.6677(16) Å, O002−H002−O9 = 166.5(2)°) with two methanol molecules, the first bridging the acetate group and the hydroxyl at C_9 and the second being linked to the phosphonic acid. The rigid chair−chair conformation of the

DOI: 10.1021/acs.inorgchem.7b01731
Inorg. Chem. XXXX, XXX, XXX−XXX

Table 2. Crystallographic Data for the Structures of 2Na, L_2, and L_3[72]

	2Na	L_2	L_3
formula	$C_{24}H_{30}N_4NaO_9P$, MeOH	$C_{21}H_{25}N_4O_8P$,2 MeOH	$C_{26}H_{30}N_4O_7$
mol wt (g mol^{-1})	604.52	556.50	510.54
temp (K)	150(2)	150(2)	173(2)
cryst size (mm)	041 × 0.24 × 0.11	0.55 × 0.49 × 0.43	0.30 × 0.25 × 0.20
cryst syst	triclinic	monoclinic	monoclinic
space group	$P\bar{1}$	$P2_1/n$	$P2_1/c$
unit cell dimens			
a (Å)	8.3045(2)	13.4531(5)	14.8091(4)
b (Å)	13.5397(5)	10.6527(3)	11.8613(4)
c (Å)	14.3175(6)	18.3216(7)	14.8551(4)
α (deg)	113.495(2)		
β (deg)	91.526(2)	92.1580(10)	100.775(2)
γ (deg)	93.495(2)		
V (Å^3); Z	1471.37(9); 2	2623.84(16);4	2563.37(13); 4
calcd density (g cm^{-3})	1.364	1.409	1.323
abs coeff (mm^{-1})	0.168	0.167	0.097
F(000)	636	1176	1080
θ_{max} (deg)	27.48	27.52	27.46
no. of rflns collected	14303	23378	25582
no. of indep rflns ($I > 2\sigma(I)$)	4964	5409	5860
no. of params	378	357	338
R1, wR2 ($I > 2\sigma(I)$)	0.0511, 0.1307	0.0367, 0.098	0.0566, 0.1418
R1, wR2 (all data)	0.0695, 0.1433	0.041, 0.1017	0.0832, 0.1555

Table 3. Selected Bond Lengths and Angles in 2, L_2, and L_3[72]

	2	L_2	L_3
	Bond Lengths (Å)		
Na−N1	2.6205(18)		
Na−N2	2.4551(15)		
Na−N3	2.4802(23)		
Na−N4	2.4917(24)		
Na−O8	2.3330(15)		
Na−O9	2.3695(18)		
N1···N2	2.9429(24)	2.6935(13)	2.888(2)
N3···N4	4.6521(31)	4.6913(16)	7.186(2)
	Angles (deg)		
Pyr1···Pyr2	144.05	116.8	159.8

bicycle was also observed in solution by ^{1}H NMR (Figure S9 in the Supporting Information) with a typical Overhauser effect between the pyridyl protons H_d and the equatorial protons H_6 (see Figure S13 in the Supporting Information for ^{1}H−^{1}H NOESY). Attempts to grow single crystals of the CuL_2 complex have also been carried out, unfortunately leading to crystals of insufficient quality for X-ray diffraction.

Thermodynamic Studies. *Protonation Constants of Ligand L_2.* Ligand L_2 (Chart 1) has five protonatable sites in the usual 2 ≤ pH ≤ 12 window in water: two tertiary amines, two carboxylic acids, and one phosphonic acid. The crystal structure of L_2 suggests that only one of the two tertiary amines is protonated. However, three potential additional protonation constants have to be taken into account at lower pH values, which account for the second protonation of the phosphonic acid and for the protonations of the two pyridine rings.[21] Protonation constants, as defined by eqs 1 and 2, were determined by a combination of potentiometric titrations (Figure S14 in the Supporting Information) and UV−visible absorption titrations versus pH between pH −0.6 and 12 (Figure 3).

$$LH_{n-1} + H \leftrightarrow LH_n \quad (1)$$

$$K_1^H = \frac{[LH_n]}{[LH_{n-1}][H]} \qquad n = 1-6 \quad (2)$$

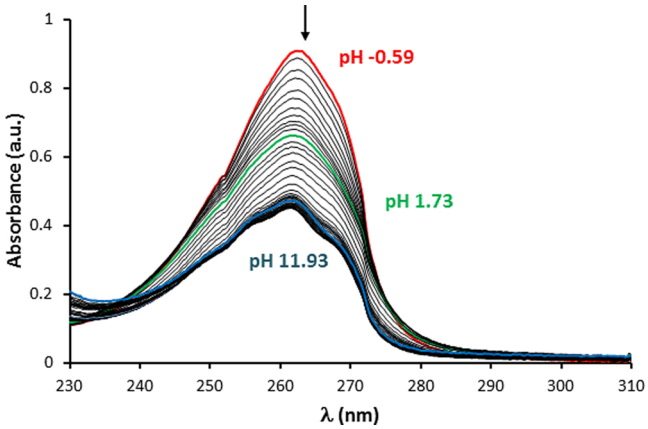

Figure 3. Spectrophotometric titrations of L_2 vs pH at −0.6 < p[H] < 1.73 (batch titration) and 2.10 ≤ pH ≤ 11.93 (direct titration). Conditions: $[L_2]_{tot} = 4.80 \times 10^{-5}$ M; solvent, H_2O; I = 0.1 M KCl; T = 25.0(2) °C.

Because of the known strong stability of the metal complexes of bispidine derivatives,[4,20] ligand L_2 and its metal complexes were also studied under strongly acidic conditions (−0.59 < pH < 1.73) by means of spectrophotometric titrations vs pH. As such a low pH cannot be measured with an electrode, the batch titration technique was used and the pH of the solutions was fixed by adding known volumes of standardized $HClO_4$ (see the Experimental Section for details). It has to be noted that the ionic strength was not fixed below pH 1 in the batch titrations and that no decomposition of the ligand was observed, even

DOI: 10.1021/acs.inorgchem.7b01731
Inorg. Chem. XXXX, XXX, XXX−XXX

under strongly acidic conditions. The spectral variations of $\mathbf{L_2}$ observed at −0.59 < pH < 1.73 (batch titration) and 2.10 < pH < 11.93 (direct titration) were combined in Figure 3. $\mathbf{L_2}$ showed one band, centered at 263 nm, attributed to the $\pi-\pi^*$ transition of the pyridine rings, which underwent a hypochromic variation with the appearance of shoulders upon an increase in the pH.[60] The hypochromic variation is typical of the deprotonation of pyridinium nitrogens, while the shoulders appearing under basic conditions suggest the existence of hydrogen bonding with at least one pyridine nitrogen lone pair.[84]

The statistical analysis of the potentiometric and spectrophotometric data versus pH was achieved with Hyperquad2008[85] and Hypspec software,[78] respectively, and led to the determination of five protonation constants of ligand $\mathbf{L_2}$ in the pH range from −0.59 to 11.93 (Table 4). The first protonation constant (log K_1^H = 11.5(3)) was assigned to the tertiary amine of the bispidine skeleton.[82,86−88] From crystallographic data, it was postulated that simultaneous protonation of the two tertiary amines does not occur. The second protonation constant (log K_2^H = 7.2(1)) was attributed to the first protonation of the phosphonic acid. The third and fourth protonation constants (K_3^H, K_4^H) were attributed to the two carboxylic acid oxygens. The two most acidic protonation constants belong to the pyridine nitrogens and/or to the second protonation of the phosphonic acid. Only one of them could be determined from our spectrophotometric batch titrations (log K_5^H = 0.5(1)). These protonation constants are in good agreement with those determined previously for ligand $\mathbf{L^1}$ and for an analogue of $\mathbf{L_2}$ bearing a thiophene group in place of the phosphonic acid.[21]

Table 4. Successive Protonation Constants of $\mathbf{L_2}$ and $\mathbf{L_1}$[a]

pK_n^H		$\mathbf{L_2}$	$\mathbf{L_1}$
pK_1^H	N_{tert}	11.5(3)	10.6(6)
pK_2^H	HPO_3^-	7.2(1)	
pK_3^H	COOH	3.8(3)	4.5(1)
pK_4^H	COOH	2.4(4)	2.0(2)
pK_5^H	PO_3^{2-}/N_{pyr}	0.5(1)	0.82(1)
pK_6^H	N_{pyr}	<0.5	<0.82

[a]Conditions: solvent, H_2O; I = 0.1 M (KCl); T = 25.0 °C. The values in parentheses correspond to the standard deviations expressed as the last significant digit.

From these values, the electronic spectra of the protonated species of $\mathbf{L_2}$ (Figure 4a) and their distribution diagram (Figure 4b) were calculated.[89] The distribution curves showed that, due to the presence of the phosphonate moiety (pK_2^H = 7.2(1)), the ligand exists in its $\mathbf{L_2H^{3-}}$ and $\mathbf{L_2H_2^{2-}}$ forms under physiological conditions (pH 7.4).

Stability Constants of the Cu(II) and Zn(II) Complexes. Spectrophotometric titrations versus pH of solutions of $\mathbf{L_2}$ and Cu(II) were carried out between pH −0.59 and 2 (batch titration) to ensure complete decomplexation of Cu(II) and between pH 2 and 12 (direct titration) both on the ligand bands and on the Cu(II) d−d bands (Figure 5). The position of the Cu(II) d−d bands at pH 2 (λ_{max} 682 nm) shows that the Cu(II) complex is already formed at this pH and suggests a square-pyramidal geometry.[90] Significant changes were seen in the UV−visible absorption spectra of $\mathbf{CuL_2}$ as a function of pH, where the hypo- and hypsochromic shifts of the main band at 260 nm together with the appearance of a small charge transfer band (Figure 5a)[61] indicated the complete formation of the complex at pH 0.2. Further spectral variations were observed between pH 2 and 12, suggesting the successive formation of different species.

Data analysis[85,78] suggested that the best model involves the successive formation of $\mathbf{CuL_2H_2}$, $\mathbf{CuL_2H}$, and $\mathbf{CuL_2}$ over the entire studied pH range (Table 5) with high stability constants. This model was confirmed by potentiometric titrations between pH 2 and 12 in which the $\mathbf{CuL_2H_2}$ stability constant, determined from the batch titration, was fixed.

We then focused our attention on the study of the complexation of Zn(II), since it is a common metallic impurity in no-carrier-added radiocopper solutions.[81] Potentiometric and spectrophotometric titrations versus pH of $\mathbf{L_2}$ with stoichiometric amounts of Zn(II) showed the same model of complexation as for Cu(II),: i.e., the successive formation of $\mathbf{ZnL_2H_2}$, $\mathbf{ZnL_2H}$, and $\mathbf{ZnL_2}$ species.

In order to compare the chelating ability of $\mathbf{L_2}$ for Cu(II) and Zn(II) with other ligands, their pM (M = Cu(II), Zn(II)) values at physiological pH (pH 7.4) were calculated (Tables 1 and 5). By representing the amount of free metal in solution at physiological pH, the pM allows a comparison of the chelation power of ligands having different denticities and protonation properties for various metals. These results indicated a very strong stability of the Cu(II) complex bearing a phosphonate arm, with a pCu value 2 orders of magnitude larger than that of the previously studied ligand $\mathbf{L_1}$ with a carboxylate arm and among the highest observed for ^{64}Cu PET ligands (Table 1).

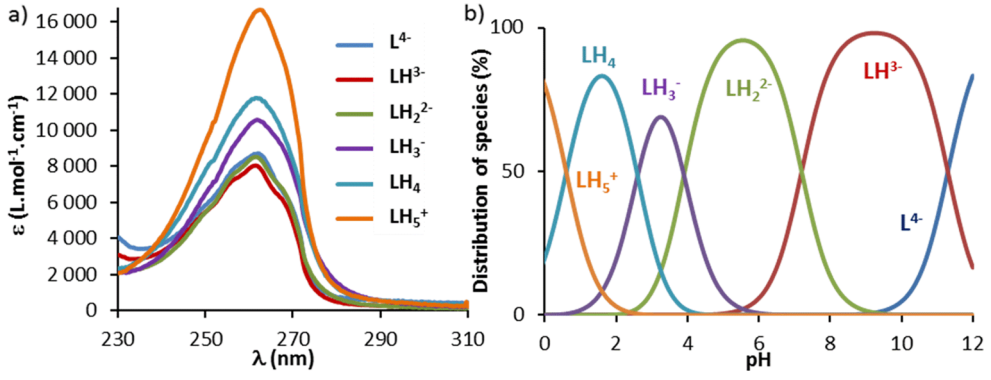

Figure 4. (a) Electronic spectra and (b) distribution diagram of the protonated species of $\mathbf{L_2}$. Conditions: $[\mathbf{L_2}]_{tot}$ = 5.0 × 10^{-5} M; solvent, H_2O; I = 0.1 M KCl; T = 25.0(2) °C.

DOI: 10.1021/acs.inorgchem.7b01731
Inorg. Chem. XXXX, XXX, XXX−XXX

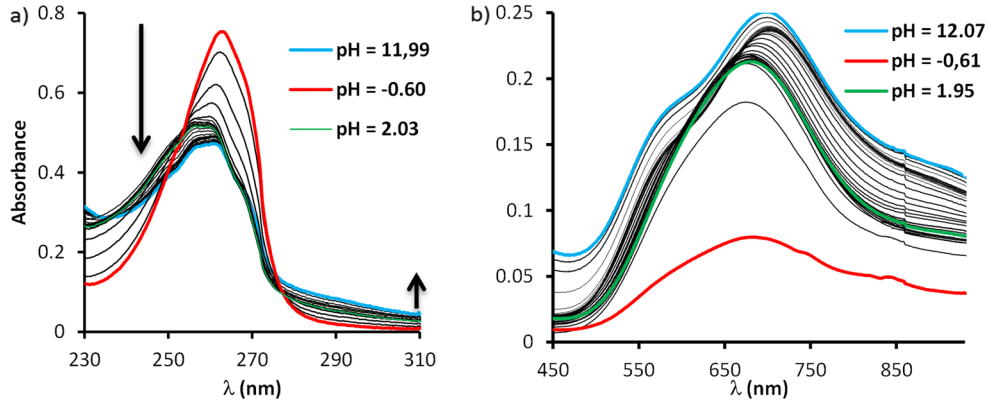

Figure 5. Spectrophotometric titration of Cu $\mathbf{L_2}$ vs pH: (a) $[\mathbf{L_2}]_{tot} = 4.79 \times 10^{-5}$ M, $[Cu(II)]_{tot}/[\mathbf{L_2}]_{tot} = 0.97$, $-0.60 < pH < 11.99$, H_2O, $I = 0.1$ M (KCl), $T = 25.0(2)$ °C; (b) $[\mathbf{L_2}]_{tot} = 2.50 \times 10^{-3}$ M, $[Cu(II)]_{tot}/[\mathbf{L_2}]_{tot} = 0.97$, $-0.61 < pH < 12.07$, H_2O, $I = 0.1$ M (KCl), $T = 25.0(2)$ °C.

Table 5. Overall Stability Constants (log β) of the ML_2 and ML_1 Complexes[a]

	Cu(II)		Zn(II)	
	$\mathbf{L_1}$	$\mathbf{L_2}$	$\mathbf{L_1}$	$\mathbf{L_2}$
log β_{ML}	19.2(3)	22.5(1)	14.45(2)	18.8(1)
pK_{a1}		4.9(3)		5.3(2)
pK_{a2}		3.1(3)		3.1(2)
pM (pH 7.4)	17.0	19.1	12.2	15.4

[a]Conditions: M = Cu(II), Zn(II); solvent, H_2O; $I = 0.1$ M; $T = 25.0$ °C; $\beta_{MLH} = [MLH]/([M][L][H])$. Charges are omitted for clarity. log $K_{Cu(OH)} = -6.29$. log $K_{Cu(OH)2} = -13.1$. log $K_{Zn(OH)} = -7.89$. log $K_{Zn(OH)2} = -14.92$ (from ref 91). pM = $-\log[M(II)_{free}]$ with $[M] = 10^{-6}$ M and $[L] = 10^{-5}$ M, pH 7.4.

Moreover, ligand $\mathbf{L_2}$ showed a good selectivity for Cu(II) in comparison to Zn(II), with a more than 3 orders of magnitude increase in pM values between the Cu(II) and Zn(II) complexes.

The electronic spectra of the Cu(II) and Zn(II) complexes of $\mathbf{L_2}$ (Figure 6a) and their species distribution profiles (Figure 6b) were calculated from their thermodynamic stability constants. The distribution curves show that, for both Cu(II) and Zn(II), the ML complex is the major species at physiological pH (pH 7.4).

pK_as of the Zn(II) complexes have been confirmed by variable-pH ^{1}H and ^{31}P NMR spectroscopy of a stoichiometric mixture of $\mathbf{L_2}$ and $ZnCl_2$ in D_2O (Figure 7). At pD 12.6, the ^{1}H NMR spectrum is consistent with the formation of a rigid 1:1 complex (Figure S15 in the Supporting Information) and all protons could be assigned by ^{1}H–^{1}H COSY and NOESY experiments (Figure S16 in the Supporting Information). Significant variations are observed in the chemical shifts of the protons H6/8 ($\Delta\delta = 0.2$ ppm) and H_e ($\Delta\delta = 0.29$ ppm), as well as of the phosphorus atom ($\Delta\delta = 4.63$ ppm) (Figure 8; see numbering in Scheme 1). The strong variations in ^{31}P and H_e suggest that the first protonation occurs on the phosphonate function and values of pK_{a1}(^{31}P) = 5.4 and pK_{a1}(H6) = 5.3 could be determined from the analysis of the chemical shift of the ^{31}P atom and proton H6, respectively (Figure 7c). These results are in very good agreement with the pK_{a1} value obtained from potentiometric and spectrophotometric titrations. Protonation of the phosphonate also influences the chemical shift of the H6/8 protons in the $4.8 \leq pH \leq 7.2$ range. Moreover, the protonation curve of $H6/8_{eq}$ clearly indicates that a second protonation reaction takes place below pH 4, which could be assigned to the protonation of a carboxylate function.

Electrochemical Studies of the Cu(II) Complexes with Ligand $\mathbf{L_2}$. In order to verify that the reduction potential of $Cu\mathbf{L_2}$ is below the threshold for in vivo reduction, estimated to −0.4 V (vs NHE),[92,93] we performed cyclic voltammetry studies at different pH (Figure 8).

At physiological pH where the $Cu\mathbf{L_2}$ species predominates, quasi-reversible processes were observed in both reduction and oxidation. A single redox couple was identified, corresponding to Cu(II)/Cu(I) ($E_{red} = -0.81$ V vs Ag/AgCl, i.e. $E_{red} = -0.60$ V vs NHE), clearly indicating the absence of demetalation and suggesting that $\mathbf{L_2}$ is able to stabilize both Cu(II) and Cu(I) in this pH range. Similar behaviors were also observed for ligand $\mathbf{L_1}$ and other bispidone derivatives[21,4] and for NO1PA2PY ($E_{red} = -0.518$ V vs NHE)[44] and CB-TE1PA ($E_{1/2} = -0.62$ vs

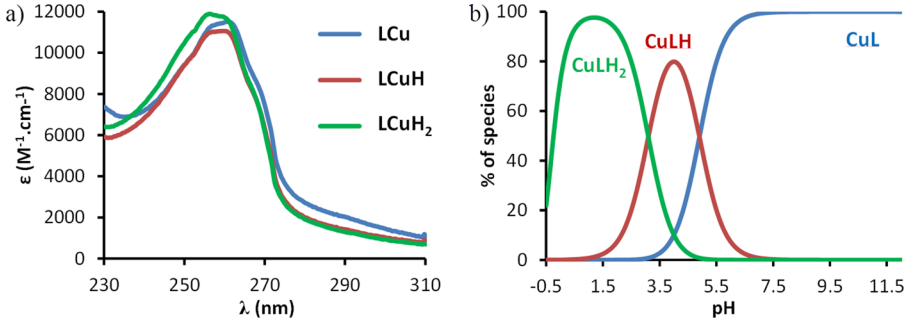

Figure 6. (a) Electronic spectra and (b) distribution diagram of the different Cu(II)-$\mathbf{L_2}$ species. Conditions: $[\mathbf{L_2}]_{tot} = 5.05 \times 10^{-5}$ M; $[Cu]_{tot}/[\mathbf{L_2}]_{tot} = 0.98$; H_2O, $I = 0.1$ M KCl; $T = 25.0(2)$ °C).

DOI: 10.1021/acs.inorgchem.7b01731
Inorg. Chem. XXXX, XXX, XXX−XXX

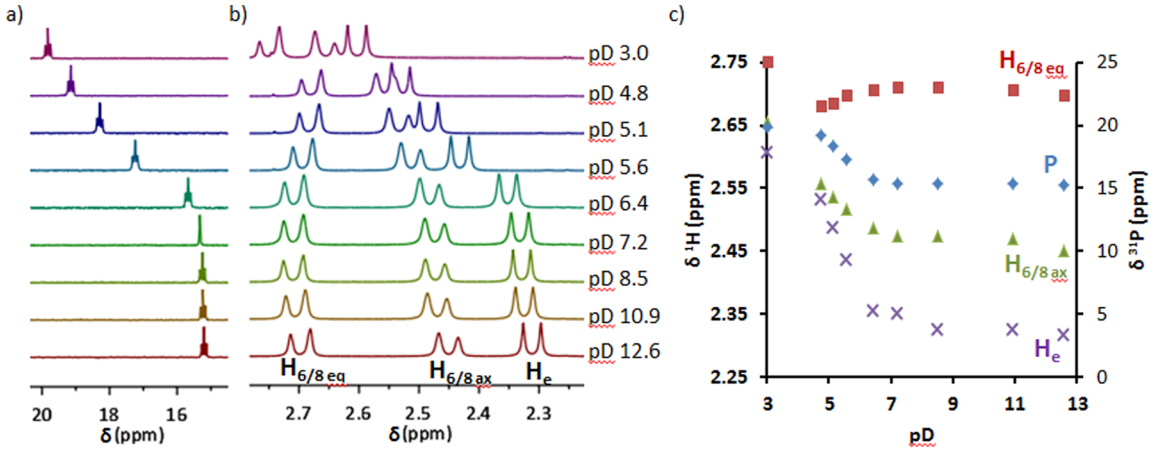

Figure 7. Variable pH NMR of a 1:1 $\mathbf{L_2}$:$ZnCl_2$ solution in D_2O at 25 °C: (a) ^{31}P NMR spectra; (b) enlargement of the ^{1}H NMR spectra in the 2.25−2.75 ppm region; (c) protonation curves f(pD) for P, H_e, and H6/8.

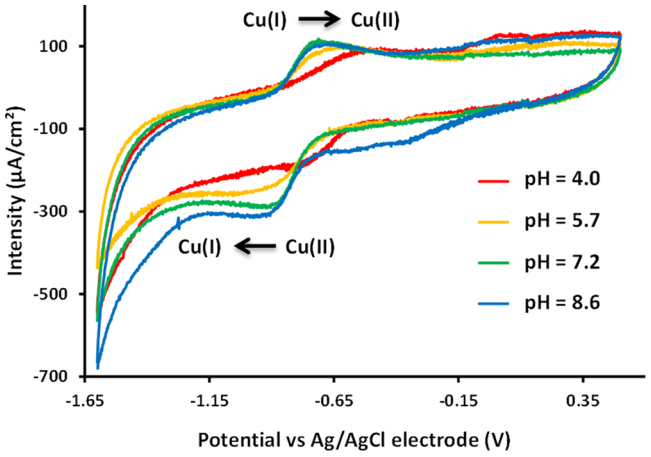

Figure 8. Cyclic voltammograms of $Cu\mathbf{L_2}$ at different pHs (V = 200 mV/s). Conditions: [$Cu\mathbf{L_2}$] = 1.09 × 10^{-3} M; solvent, H_2O; I = 0.1 M ($NaClO_4$); T = 25.0(2) °C.

NHE).[94] Quasi-reversibility was also verified by measuring the peak anodic (i_{pa}) and cathodic (i_{pc}) currents with varying scan speed (v) at fixed pH. The linear plots of i_{pa} or $i_{pc} = f(v^{1/2})$ are shown in Figure S17 in the Supporting Information. The E_{red} value is similar to the value obtained for ligand $\mathbf{L_1}$ (E_{red} = −0.56 V) and is well below the estimated −0.40 V (vs NHE) threshold for typical bioreductants[30] and below those of Cu(II) complexes with bispidones $\mathbf{L_0}$ (E_{red} = −0.323 V vs NHE) and **HZ2** (E_{red} = −0.225 V vs NHE).[4] More stable bispidine ligands have been reported more recently; however, redox potentials were measured in organic solvents such as DMF (E_{red} = −1.17 V vs fc/fc^+, i.e. E_{red} = −0.72 V vs NHE for [Cu(bispa^{1b})]$^+$) and acetonitrile (E_{red} = −0.66 V vs fc/fc^+, i.e. E_{red} = −0.26 V vs NHE for [Cu(N2py4)]$^{2+}$) and therefore cannot be compared with our system.[83] With such a low redox potential, the $Cu\mathbf{L_2}$ complex should not be subject to reduction, demetalation, or dismutation under physiological conditions. Below pH 5 and above pH 8.5 more complex phenomena were observed (Figure S18 in the Supporting Information), in accordance with the distribution curves showing the presence of other chemical species.

Kinetic Inertness of $Cu\mathbf{L_2}H_2$ in Strongly Acidic Media. Good candidates for radiopharmaceutical applications exhibit strong stability at physiological pH and in reductive medium

good selectivity, but more importantly, high kinetic inertness toward dissociation.[95] The kinetic inertness of a complex is commonly evaluated by following its acid-assisted dissociation under strongly acidic conditions under pseudo-first-order conditions. Providing all other criteria were satisfied, the obtained half-life was shown to be a good gauge of the in vivo stability of ^{64}Cu-labeled chelates.[96] The decomplexation of the $Cu\mathbf{L_2}H_2$ complex in 5 M $HClO_4$ aqueous solutions at 25 °C was followed by UV−visible absorption spectrophotometry on both the ligand π−π^* transitions and the Cu(II) d−d bands over a period of 20 months. Very minor decomplexation is observed within the period, as assessed by the slight decrease of the absorption spectrum of the d−d transitions (only 6.4% at 670 nm; Figure S19 in the Supporting Information), which indicates a higher degree of inertness of the complex in comparison to the preciously studied $Cu\mathbf{L_1}$ ($t_{1/2}$ = 110 days) under the same conditions.

Radiolabeling Studies. The high stability of the Cu(II) complex prompted us to study the radiolabeling efficiency of ligand $\mathbf{L_2}$ with $^{64}CuCl_2$ in 0.1 M ammonium acetate buffer at room temperature (Figure 9). ^{64}Cu sources of different specific

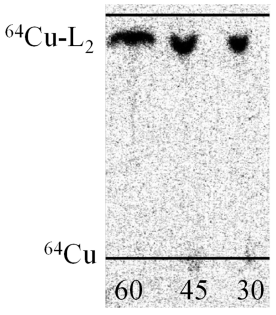

Figure 9. Thin-layer radiochromatogram of ^{64}Cu-$\mathbf{L_2}$ after 30, 45, and 60 min reaction time at pH 5.4 at room temperature in 0.1 M NH_4OAc (SiO_2, aqueous NH_3/MeOH/H_2O 1/2/1).

activities and cold metal impurities were used. For each experiment, the total concentration in metals ([M]) of the batch used was taken into account. Two series of measurements were performed in order to optimize the radiolabeling conditions. On the one hand, the influence of the ligand to metal ratio was investigated at a fixed pH of 5.4, and on the

DOI: 10.1021/acs.inorgchem.7b01731
Inorg. Chem. XXXX, XXX, XXX−XXX

other hand, the influence of pH (i.e., pH 2−7) was studied for a fixed L/M ratio.

Quantitative radiolabeling was achieved for ligand $\mathbf{L_2}$ after 30 min at room temperature with L/M ratios of 1.25 and above (Figure 10). In the presence of a substoichiometric amount of

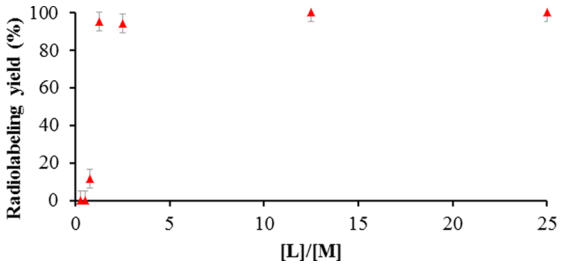

Figure 10. Radiolabeling yields of L_2 (red ▲) at different ligand/metal ratios. Conditions: 0.1 M NH_4OAc; pH 5.4; room temperature; 30 min; ^{64}Cu from batch 1; 0.12 nmol ≤ n(ligand) ≤ 12.0 nmol; n(Cu) = 8.04 pmol.

ligand, radiolabeling did not occur at room temperature (Table 6). This might be explained by a slower kinetics of the

Table 6. Time Dependence of the ^{64}Cu Radiolabeling Yields for L_2 at Different Metal/Ligand Ratios[a]

	t (min)					
L/M	5	10	15	30	45	60
0.25	0	0	0	0	0	0
0.5	0	0	0	0	0	0
0.75	0	0	0	12	11	11
1.25	≥95[b]	≥95[b]	≥95[b]	95	96	94
2.5	92	93	93	94	92	100
12.5	≥95[b]	≥95[b]	≥95[b]	100	100	100
25	100	100	100	100	100	100

[a]Conditions: 0.1 M NH_4OAc; pH 5.4; room temperature; ^{64}Cu from batch 1; 0.12 nmol ≤ n(ligand) ≤ 12.0 nmol; n(Cu) = 8.04 pmol. [b]No free Cu(II) was seen on radio-TLCs.

radiolabeling reaction, due to the presence of competitive metal salts (in particular, Fe(II/III) was present at a concentration of 6.38 ppm in batch 1, which is relatively high for such production and purification processes). However, after incubation of the samples at 80 °C for 1 h, the ^{64}Cu-$\mathbf{L_2}$ complex was formed in 4%, 5%, and 22% yields for $\mathbf{L_2}$/M ratios of 0.25, 0.5, and 0.75, respectively, at 80 °C, which indicate a thermodynamic selectivity of $\mathbf{L_2}$ for Cu(II) over the other cations. Moreover, very efficient radiolabeling (up to 95%) was achieved within 30 min at room temperature and with $\mathbf{L_2}$/M ratios of only 1.25. In the presence of a larger excess of ligand (25 equiv), quantitative radiolabeling was achieved within only 5 min. Under similar conditions, the radiochemical yield of ligand $\mathbf{L_1}$ leveled at about 90%. In the case of $\mathbf{L_4}$ and $\mathbf{L_5}$ (Chart 2), radiochemical yields of 95% were obtained at room temperature with a large excess of ligand (10^{-4} M). These results indicate a better radiolabeling capacity of the phosphonate derivative $\mathbf{L_2}$ over the carboxylate and the pyridyl analogues, which is partially explained by the stronger thermodynamic stability of the copper(II) complex with $\mathbf{L_2}$ (Table 6).

The influence of the pH was also investigated in the range 2.1−6.6 (Table 7 and Figure 11). The results indicate that pH control is mandatory for ligand $\mathbf{L_2}$, the reaction kinetics being

Table 7. Time Dependence of the Radiolabeling Yields of L_2 at Different pH Values[a]

	t (min)					
pH	5	10	15	30	45	60
2.1	36	40	49	61	70	74
3.3	60	70		87	89	90
4.6	≥95[b]	≥95[b]	≥95[b]			
5.4	≥95[b]	≥95[b]	≥95[b]	95	96	94
6.6	≥95[b]	≥95[b]	≥95[b]	100	100	100

[a]Conditions: room temperature; 0.1 M NH_4OAc; ^{64}Cu from batch 1 (pH 2.1−4.6), n(ligand) = 0.6 nm, n(Cu) = 8.04 pmol, ^{64}Cu from batch 2 (pH 4.6-6.6), n(ligand) = 0.11 nmol, n(Cu) = 22.4 pmol; L/M = 1.25. [b]No free Cu(II) was seen on radio-TLCs.

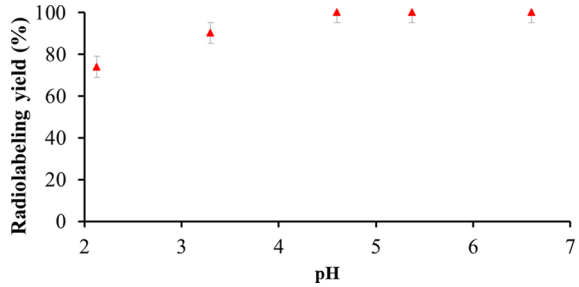

Figure 11. Radiolabeling yields of L_2 (red ▲) at different pH values. Conditions: room temperature; 0.1 M NH_4OAc; 15 min; ^{64}Cu from batch 1 (pH 2.1−4.6), n(ligand) = 0.6 nm, n(Cu) = 8.04 pmol; ^{64}Cu from batch 2 (pH 4.6−6.6), n(ligand) = 0.11 nmol, n(Cu) = 22.4 pmol; L/M = 1.25. No free Cu(II) was seen on radio-TLCs.

significantly slower under acidic conditions, probably due to the competition with the protonated species $\mathbf{L_2H_3}$, as emphasized by potentiometric and X-ray crystallographic data. However, above pH 5.4, an efficient and quantitative radiolabeling was achieved at room temperature. With quantitative radiolabeling at ligand concentrations as low as 2×10^{-7} M, we believe that $\mathbf{L_2}$ is a promising system for the complexation of ^{64}Cu and that it is worth investigating its in vivo behavior in further studies.

CONCLUSION

In conclusion, the phosphonate pendant-armed bispidol ligand $\mathbf{L_2}$ was easily synthesized in three steps from piperidinone and (aminomethyl)phosphonic acid. The evaluation of the physicochemical properties of the corresponding Cu(II) and Zn(II) complexes in water using UV−visible absorption spectrophotometry, potentiometry, ^{1}H and ^{31}P NMR, and cyclic voltammetry as well as radiolabeling experiments with $^{64}Cu^{II}$ has been reported. Fast complexation of Cu(II) occurs in the pH 4.6−6.6 range, and the complex demonstrates a strong thermodynamic stability (log β_{CuL2} = 22.5, pCu = 19.1 at pH 7.4) and a good selectivity for Cu(II) vs. Zn(II) (pZn = 15.4 at pH 7.4), as well as a very good kinetic inertness regarding reduction (with a reversible redox potential of E_{red} = −0.60 vs NHE) and acid-assisted dissociation ($t_{1/2} \gg 20$ months). Quantitative radiolabeling (100% ± 5%) was achieved within 5 min at room temperature at pH above 5.4 at ligand concentrations as low as 2×10^{-7} M. From a coordination chemistry point of view, we believe that $\mathbf{L_2}$ meets all the required criteria to be used as a new chelator for PET imaging with ^{64}Cu. Although it is out of the scope of the present paper, in vitro and in vivo stability studies as well as biodistribution studies are still needed to validate the potential of $\mathbf{L_2}$ for ^{64}Cu-

DOI: 10.1021/acs.inorgchem.7b01731
Inorg. Chem. XXXX, XXX, XXX−XXX

immuno PET imaging. Several functionalization strategies are currently being studied in order to obtain bifunctional ligands conjugated to antibodies.

■ ASSOCIATED CONTENT

Supporting Information

The Supporting Information is available free of charge on the ACS Publications website at DOI: 10.1021/acs.inorgchem.7b01731.

1D and 2D NMR spectra, plots of potentiometric titration data, plot showing the influence of scan speed on current intensity at pH 7.4, cyclic voltammograms of CuL_2 at various pHs, and plot of the evolution of the absorption spectra of the d−d transition on CuL_2H_2 in 5 M $HClO_4$ over 20 months at 25 °C (PDF)

Accession Codes

CCDC 1530205−1530206 contain the supplementary crystallographic data for this paper. These data can be obtained free of charge via www.ccdc.cam.ac.uk/data_request/cif, or by emailing data_request@ccdc.cam.ac.uk, or by contacting The Cambridge Crystallographic Data Centre, 12 Union Road, Cambridge CB2 1EZ, UK; fax: +44 1223 336033.

■ AUTHOR INFORMATION

Corresponding Authors

*E-mail for A.M.N.: aline.nonat@unistra.fr.
*E-mail for L.J.C.: l.charbonn@unistra.fr..

ORCID

Aline M. Nonat: 0000-0003-0478-5039
Loïc J. Charbonnière: 0000-0003-0328-9842

Notes

The authors declare no competing financial interest.

■ ACKNOWLEDGMENTS

This work was supported by the by the French Centre National de la Recherche Scientifique and the University of Strasbourg (UMR7178). The authors thank Mourad Elhabiri (Laboratoire de Chimie Médicinale et Bioorganique, UMR 7509 CNRS/UdS) for providing the facilities for cyclic voltammetry experiments as well as for thoughtful discussions. R.G. thanks the French Ministry of research and higher education for financial support for his Ph.D. The ARRONAX cyclotron is a project promoted by the Regional Council of Pays de la Loire, financed by local authorities, the French government, and the European Union. This work has been, in part, supported by the French National Agency for Research ("Investissements d'Avenir" research grant Equipex Arronax-Plus no. ANR-11-EQPX-0004 and Labex no. ANR-11-LABX-0018-01) and Labex IRON.

■ REFERENCES

(1) Comba, P.; Kerscher, M.; Schiek, W.; Karlin, K. D. Bispidine Coordination Chemistry. *Prog. Inorg. Chem.* **2007**, *55*, 613−704.

(2) Haller, R. Metal chelates of pyridyl-(2)-substituted 3,7-diazabicyclo-(3,3,1)-nonanones. *Arch. Pharm.* **1969**, *302* (2), 113−118.

(3) Börzel, H.; Comba, P.; Hagen, K. S.; Lampeka, Y. D.; Lienke, A.; Linti, G.; Merz, M.; Pritzkow, H.; Tsymbal, L. V. Iron Coordination Chemistry with Tetra-, Penta- and Hexadentate Bispidine-Type Ligands. *Inorg. Chim. Acta* **2002**, *337*, 407−419.

(4) Born, K.; Comba, P.; Ferrari, R.; Lawrance, G. A.; Wadepohl, H. Stability Constants: A New Twist in Transition Metal Bispidine Chemistry. *Inorg. Chem.* **2007**, *46* (2), 458−464.

(5) Comba, P.; Kerscher, M.; Merz, M.; Müller, V.; Pritzkow, H.; Remenyi, R.; Schiek, W.; Xiong, Y. Structural Variation in Transition-Metal Bispidine Compounds. *Chem. - Eur. J.* **2002**, *8* (24), 5750−5760.

(6) Bukowski, M. R.; Comba, P.; Lienke, A.; Limberg, C.; Lopez de Laorden, C.; Mas-Ballesté, R.; Merz, M.; Que, L. Catalytic Epoxidation and 1,2-Dihydroxylation of Olefins with Bispidine−Iron(II)/H_2O_2 Systems. *Angew. Chem., Int. Ed.* **2006**, *45* (21), 3446−3449.

(7) Born, K.; Comba, P.; Daubinet, A.; Fuchs, A.; Wadepohl, H. Catecholase Activity of Dicopper(II)-Bispidine Complexes: Stabilities and Structures of Intermediates, Kinetics and Reaction Mechanism. *JBIC, J. Biol. Inorg. Chem.* **2006**, *12* (1), 36−48.

(8) Comba, P.; Haaf, C.; Lienke, A.; Muruganantham, A.; Wadepohl, H. Synthesis, Structure, and Highly Efficient Copper-Catalyzed Aziridination with a Tetraaza-Bispidine Ligand. *Chem. - Eur. J.* **2009**, *15* (41), 10880−10887.

(9) Zayya, A. I.; Spencer, J. L. Coordination Chemistry of a Bicyclic 3-Aza-7-Phosphabicyclo[3.3.1]-Nonan-9-One Ligand. *Organometallics* **2012**, *31* (7), 2841−2853.

(10) Scharnagel, D.; Müller, A.; Prause, F.; Eck, M.; Goller, J.; Milius, W.; Breuning, M. The First Modular Route to Core-Chiral Bispidine Ligands and Their Application in Enantioselective Copper(II)-Catalyzed Henry Reactions. *Chem. - Eur. J.* **2015**, *21* (35), 12488−12500.

(11) Barman, P.; Vardhaman, A. K.; Martin, B.; Wörner, S. J.; Sastri, C. V.; Comba, P. Influence of Ligand Architecture on Oxidation Reactions by High-Valent Nonheme Manganese Oxo Complexes Using Water as a Source of Oxygen. *Angew. Chem., Int. Ed.* **2015**, *54* (7), 2095−2099.

(12) Ang, W. J.; Chng, Y. S.; Lam, Y. luorous Bispidine: A Bifunctional Reagent for Copper-Catalyzed Oxidation and Knoevenagel Condensation Reactions in Water. *RSC Adv.* **2015**, *5* (99), 81415−81428.

(13) Bautz, J.; Comba, P.; Que, L. Spin-Crossover in an Iron(III)−Bispidine−Alkylperoxide System. *Inorg. Chem.* **2006**, *45* (18), 7077−7082.

(14) Atanasov, M.; Busche, C.; Comba, P.; El Hallak, F.; Martin, B.; Rajaraman, G.; van Slageren, J.; Wadepohl, H. Trinuclear {M1}CN-{M2}2 Complexes (M1 = CrIII, FeIII, CoIII; M2 = CuII, NiII, MnII). Are Single Molecule Magnets Predictable? *Inorg. Chem.* **2008**, *47* (18), 8112−8125.

(15) Atanasov, M.; Comba, P.; Helmle, S. Cyanide-Bridged FeIII−CuII Complexes: Jahn−Teller Isomerism and Its Influence on the Magnetic Properties. *Inorg. Chem.* **2012**, *51* (17), 9357−9368.

(16) Kolanowski, J. L.; Jeanneau, E.; Steinhoff, R.; Hasserodt, J. Bispidine Platform Grants Full Control over Magnetic State of Ferrous Chelates in Water. *Chem. - Eur. J.* **2013**, *19* (27), 8839−8849.

(17) Comba, P.; Rudolf, H.; Wadepohl, H. Synthesis and Transition Metal Coordination Chemistry of a Novel Hexadentate Bispidine Ligand. *Dalton Trans.* **2015**, *44* (6), 2724−2736.

(18) Juran, S.; Walther, M.; Stephan, H.; Bergmann, R.; Steinbach, J.; Kraus, W.; Emmerling, F.; Comba, P. Hexadentate Bispidine Derivatives as Versatile Bifunctional Chelate Agents for Copper(II) Radioisotopes. *Bioconjugate Chem.* **2009**, *20* (2), 347−359.

(19) Comba, P.; Hunoldt, S.; Morgen, M.; Pietzsch, J.; Stephan, H.; Wadepohl, H. Optimization of Pentadentate Bispidines as Bifunctional Chelators for ^{64}Cu Positron Emission Tomography (PET). *Inorg. Chem.* **2013**, *52* (14), 8131−8143.

(20) Comba, P.; Kubeil, M.; Pietzsch, J.; Rudolf, H.; Stephan, H.; Zarschler, K. Bispidine Dioxotetraaza Macrocycles: A New Class of Bispidines for 64Cu PET Imaging. *Inorg. Chem.* **2014**, *53* (13), 6698−6707.

(21) Roux, A.; Nonat, A. M.; Brandel, J.; Hubscher-Bruder, V.; Charbonnière, L. J. Kinetically Inert Bispidol-Based Cu(II) Chelate for Potential Application to 64/67Cu Nuclear Medicine and Diagnosis. *Inorg. Chem.* **2015**, *54* (9), 4431−4444.

(22) Brasse, D.; Nonat, A. Radiometals: Towards a New Success Story in Nuclear Imaging? *Dalton Trans.* **2015**, *44* (11), 4845−4858.

(23) Adumeau, P.; Sharma, S. K.; Brent, C.; Zeglis, B. M. Site-Specifically Labeled Immunoconjugates for Molecular Imaging—Part

DOI: 10.1021/acs.inorgchem.7b01731
Inorg. Chem. XXXX, XXX, XXX−XXX

1: Cysteine Residues and Glycans. *Mol. Imaging Biol.* **2016**, *18* (1), 1−17.
(24) Adumeau, P.; Sharma, S. K.; Brent, C.; Zeglis, B. M. Site-Specifically Labeled Immunoconjugates for Molecular Imaging—Part 2: Peptide Tags and Unnatural Amino Acids. *Mol. Imaging Biol.* **2016**, *18* (2), 153−165.
(25) England, C. G.; Hernandez, R.; Eddine, S. B. Z.; Cai, W. Molecular Imaging of Pancreatic Cancer with Antibodies. *Mol. Pharmaceutics* **2016**, *13* (1), 8−24.
(26) Sehlin, D.; Fang, X. T.; Cato, L.; Antoni, G.; Lannfelt, L.; Syvänen, S. Antibody-Based PET Imaging of Amyloid Beta in Mouse Models of Alzheimer's Disease. *Nat. Commun.* **2016**, *7*, 10759.
(27) Wu, A. M. Antibodies and Antimatter: The Resurgence of Immuno-PET. *J. Nucl. Med.* **2008**, *50* (1), 2−5.
(28) Steiner, M.; Neri, D. Antibody-Radionuclide Conjugates for Cancer Therapy: Historical Considerations and New Trends. *Clin. Cancer Res.* **2011**, *17* (20), 6406−6416.
(29) Kaur, S.; Venktaraman, G.; Jain, M.; Senapati, S.; Garg, P. K.; Batra, S. K. Recent Trends in Antibody-Based Oncologic Imaging. *Cancer Lett.* **2012**, *315* (2), 97−111.
(30) Wadas, T. J.; Wong, E. H.; Weisman, G. R.; Anderson, C. J. Coordinating Radiometals of Copper, Gallium, Indium, Yttrium, and Zirconium for PET and SPECT Imaging of Disease. *Chem. Rev.* **2010**, *110* (5), 2858−2902.
(31) Shokeen, M.; Anderson, C. J. Molecular Imaging of Cancer with Copper-64 Radiopharmaceuticals and Positron Emission Tomography (PET). *Acc. Chem. Res.* **2009**, *42* (7), 832−841.
(32) Price, E. W.; Orvig, C. Matching Chelators to Radiometals for Radiopharmaceuticals. *Chem. Soc. Rev.* **2014**, *43* (1), 260−290.
(33) Price, T. W.; Greenman, J.; Stasiuk, G. J. Current Advances in Ligand Design for Inorganic Positron Emission Tomography Tracers Ga-68, Cu-64, Zr-89 and Sc-44. *Dalton Trans.* **2016**, *45* (40), 15702−15724.
(34) Bandara, N.; Sharma, A. K.; Krieger, S.; Schultz, J. W.; Han, B. H.; Rogers, B. E.; Mirica, L. M. Evaluation of ^{64}Cu-Based Radiopharmaceuticals That Target Aβ Peptide Aggregates as Diagnostic Tools for Alzheimer's Disease. *J. Am. Chem. Soc.* **2017**, DOI: 10.1021/jacs.7b05937.
(35) Cooper, M. S.; Ma, M. T.; Sunassee, K.; Shaw, K. P.; Williams, J. D.; Paul, R. L.; Donnelly, P. S.; Blower, P. J. Comparison of ^{64}Cu-Complexing Bifunctional Chelators for Radioimmunoconjugation: Labeling Efficiency, Specific Activity, and in Vitro/in Vivo Stability. *Bioconjugate Chem.* **2012**, *23* (5), 1029−1039.
(36) Zhang, Y.; Hong, H.; Engle, J. W.; Bean, J.; Yang, Y.; Leigh, B. R.; Barnhart, T. E.; Cai, W. Positron Emission Tomography Imaging of CD105 Expression with a 64 Cu-Labeled Monoclonal Antibody: NOTA Is Superior to DOTA. *PLoS One* **2011**, *6* (12), e28005.
(37) Anderson, C. J.; Dehdashti, F.; Cutler, P. D.; Schwarz, S. W.; Laforest, R.; Bass, L. A.; Lewis, J. S.; McCarthy, D. W. ^{64}Cu-TETA-Octreotide as a PET Imaging Agent for Patients with Neuroendocrine Tumors. *J. Nucl. Med.* **2001**, *42* (2), 213−221.
(38) Pandya, D. N.; Kim, J. Y.; Park, J. C.; Lee, H.; Phapale, P. B.; Kwak, W.; Choi, T. H.; Cheon, G. J.; Yoon, Y.-R.; Yoo, J. Revival of TE2A; a Better Chelate for Cu(II) Ions than TETA? *Chem. Commun.* **2010**, *46* (20), 3517−3519.
(39) Pandya, D. N.; Bhatt, N.; Dale, A. V.; Kim, J. Y.; Lee, H.; Ha, Y. S.; Lee, J.-E.; An, G. I.; Yoo, J. New Bifunctional Chelator for 64Cu-Immuno-Positron Emission Tomography. *Bioconjugate Chem.* **2013**, *24* (8), 1356−1366.
(40) Lima, L. M. P.; Esteban-Gómez, D.; Delgado, R.; Platas-Iglesias, C.; Tripier, R. Monopicolinate Cyclen and Cyclam Derivatives for Stable Copper(II) Complexation. *Inorg. Chem.* **2012**, *51* (12), 6916−6927.
(41) Frindel, M.; Camus, N.; Rauscher, A.; Bourgeois, M.; Alliot, C.; Barré, L.; Gestin, J.-F.; Tripier, R.; Faivre-Chauvet, A. Radiolabeling of HTE1PA: A New Monopicolinate Cyclam Derivative for Cu-64 Phenotypic Imaging. In Vitro and in Vivo Stability Studies in Mice. *Nucl. Med. Biol.* **2014**, *41*, e49−e57.
(42) Frindel, M.; Camus, N.; Rauscher, A.; Bourgeois, M.; Alliot, C.; Barre, L.; Gestin, J.-F.; Tripier, R.; Faivre-Chauvet, A. Radiolabeling of HTE1PA: A New Monopicolinate Cyclam Derivative for Cu-64 Phenotypic Imaging. In Vitro and in Vivo Stability Studies in Mice. *Nucl. Med. Biol.* **2014**, *41* (Suppl), e49−57.
(43) Frindel, M.; Le Saëc, P.; Beyler, M.; Navarro, A.-S.; Saï-Maurel, C.; Alliot, C.; Chérel, M.; Gestin, J.-F.; Faivre-Chauvet, A.; Tripier, R. Cyclam Te1pa for ^{64} Cu PET Imaging. Bioconjugation to Antibody, Radiolabeling and Preclinical Application in Xenografted Colorectal Cancer. *RSC Adv.* **2017**, *7* (15), 9272−9283.
(44) Roger, M.; Lima, L. M. P.; Frindel, M.; Platas-Iglesias, C.; Gestin, J.-F.; Delgado, R.; Patinec, V.; Tripier, R. Monopicolinate-Dipicolyl Derivative of Triazacyclononane for Stable Complexation of Cu^{2+} and $^{64}Cu^{2+}$. *Inorg. Chem.* **2013**, *52* (9), 5246−5259.
(45) Guillou, A.; Lima, L. M. P.; Roger, M.; Esteban-Gòmez, D.; Delgado, R.; Platas-Iglesias, C.; Patinec, V.; Tripier, R. 1,4,7-Triazacyclononane-Based Bifunctional Picolinate Ligands for Efficient Copper Complexation: 1,4,7-Triazacyclononane-Based Bifunctional Picolinate Ligands for Efficient Copper Complexation. *Eur. J. Inorg. Chem.* **2017**, *2017* (18), 2435−2443.
(46) Boros, E.; Rybak-Akimova, E.; Holland, J. P.; Rietz, T.; Rotile, N.; Blasi, F.; Day, H.; Latifi, R.; Caravan, P. Pycup? A Bifunctional, Cage-like Ligand for ^{64} Cu Radiolabeling. *Mol. Pharmaceutics* **2014**, *11* (2), 617−629.
(47) Wadas, T. J.; Anderson, C. J. Radiolabeling of TETA- and CB-TE2A-Conjugated Peptides with Copper-64. *Nat. Protoc.* **2007**, *1* (6), 3062−3068.
(48) Esteves, C. V.; Lamosa, P.; Delgado, R.; Costa, J.; Désogère, P.; Rousselin, Y.; Goze, C.; Denat, F. Remarkable Inertness of Copper(II) Chelates of Cyclen-Based Macrobicycles with Two *Trans - N* -Acetate Arms. *Inorg. Chem.* **2013**, *52* (9), 5138−5153.
(49) Ferdani, R.; Stigers, D. J.; Fiamengo, A. L.; Wei, L.; Li, B. T. Y.; Golen, J. A.; Rheingold, A. L.; Weisman, G. R.; Wong, E. H.; Anderson, C. J. Synthesis, Cu(II) Complexation, ^{64}Cu-Labeling and Biological Evaluation of Cross-Bridged Cyclam Chelators with Phosphonate Pendant Arms. *Dalton Trans.* **2012**, *41* (7), 1938−1950.
(50) Zeng, D.; Ouyang, Q.; Cai, Z.; Xie, X.-Q.; Anderson, C. J. New Cross-Bridged Cyclam Derivative CB-TE1K1P, an Improved Bifunctional Chelator for Copper Radionuclides. *Chem. Commun.* **2014**, *50* (1), 43−45.
(51) Dale, A. V.; An, G. I.; Pandya, D. N.; Ha, Y. S.; Bhatt, N.; Soni, N.; Lee, H.; Ahn, H.; Sarkar, S.; Lee, W.; Huynh, P. T.; Kim, J. Y.; Gwon, M.-R.; Kim, S. H.; Park, J. G.; Yoon, Y.-R.; Yoo, J. Synthesis and Evaluation of New Generation Cross-Bridged Bifunctional Chelator for 64Cu Radiotracers. *Inorg. Chem.* **2015**, *54* (17), 8177−8186.
(52) Bhatt, N.; Soni, N.; Ha, Y. S.; Lee, W.; Pandya, D. N.; Sarkar, S.; Kim, J. Y.; Lee, H.; Kim, S. H.; An, G. I.; Yoo, J. Phosphonate Pendant Armed Propylene Cross-Bridged Cyclam: Synthesis and Evaluation as a Chelator for Cu-64. *ACS Med. Chem. Lett.* **2015**, *6* (11), 1162−1166.
(53) Boros, E.; Cawthray, J. F.; Ferreira, C. L.; Patrick, B. O.; Adam, M. J.; Orvig, C. Evaluation of the H2dedpa Scaffold and Its CRGDyK Conjugates for Labeling with 64Cu. *Inorg. Chem.* **2012**, *51* (11), 6279−6284.
(54) Ramogida, C. F.; Boros, E.; Patrick, B. O.; Zeisler, S. K.; Kumlin, J.; Adam, M. J.; Schaffer, P.; Orvig, C. Evaluation of H_2CHXdedpa, H_2Dedpa- and H_2CHXdedpa-N,N′-Propyl-2-NI Ligands for ^{64}Cu(II) Radiopharmaceuticals. *Dalton Trans* **2016**, *45* (33), 13082−13090.
(55) Di Bartolo, N.; Sargeson, A. M.; Smith, S. V. New Cu-64 PET Imaging Agents for Personalised Medicine and Drug Development Using the Hexa-Aza Cage, SarAr. *Org. Biomol. Chem.* **2006**, *4* (17), 3350−3357.
(56) Paterson, B. M.; Buncic, G.; McInnes, L. E.; Roselt, P.; Cullinane, C.; Binns, D. S.; Jeffery, C. M.; Price, R. I.; Hicks, R. J.; Donnelly, P. S. Bifunctional ^{64}Cu-Labelled Macrobicyclic Cage Amine Isothiocyanates for Immuno-Positron Emission Tomography. *Dalton Trans.* **2015**, *44* (11), 4901−4909.
(57) Di Bartolo, N. M.; Sargeson, A. M.; Donlevy, T. M.; Smith, S. V. Synthesis of a New Cage Ligand, SarAr, and Its Complexation with

DOI: 10.1021/acs.inorgchem.7b01731
Inorg. Chem. XXXX, XXX, XXX−XXX

Selected Transition Metal Ions for Potential Use in Radioimaging. *J. Chem. Soc., Dalton Trans.* **2001**, No. 15, 2303−2309.
(58) Roux, A.; Gillet, R.; Huclier-Markai, S.; Ehret-Sabatier, L.; Charbonnière, L. J.; Nonat, A. M. Bifunctional Bispidine Derivatives for Copper-64 Labelling and Positron Emission Tomography. *Org. Biomol. Chem.* **2017**, *15* (6), 1475−1483.
(59) Lukeš, I.; Kotek, J.; Vojtíšek, P.; Hermann, P. Complexes of Tetraazacycles Bearing Methylphosphinic/Phosphonic Acid Pendant Arms with Copper(II), Zinc(II) and Lanthanides(III). A Comparison with Their Acetic Acid Analogues. *Coord. Chem. Rev.* **2001**, *216−217*, 287−312.
(60) Abada, S.; Lecointre, A.; Déchamps-Olivier, I.; Platas-Iglesias, C.; Christine, C.; Elhabiri, M.; Charbonniere, L. Highly Stable Acyclic Bifunctional Chelator for ^{64}Cu PET Imaging. *Radiochim. Acta* **2011**, *99* (10), 663−678.
(61) Abada, S.; Lecointre, A.; Christine, C.; Ehret-Sabatier, L.; Saupe, F.; Orend, G.; Brasse, D.; Ouadi, A.; Hussenet, T.; Laquerrière, P.; Elhabiri, M.; Charbonnière, L. J. Phosphonated Chelates for Nuclear Imaging. *Org. Biomol. Chem.* **2014**, *12* (47), 9601−9620.
(62) Abada, S.; Lecointre, A.; Elhabiri, M.; Charbonnière, L. J. Formation of Very Stable and Selective Cu(II) Complexes with a Non-Macrocyclic Ligand: Can Basicity Rival Pre-Organization? *Dalton Trans.* **2010**, *39* (38), 9055−9062.
(63) Ferreira, C. L.; Yapp, D. T.; Lamsa, E.; Gleave, M.; Bensimon, C.; Jurek, P.; Kiefer, G. E. Evaluation of Novel Bifunctional Chelates for the Development of Cu-64-Based Radiopharmaceuticals. *Nucl. Med. Biol.* **2008**, *35* (8), 875−882.
(64) Bevilacqua, A.; Gelb, R. I.; Hebard, W. B.; Zompa, L. J. Equilibrium and Thermodynamic Study of the Aqueous Complexation of 1,4,7-Triazacyclononane-N,N',N''-Triacetic Acid with Protons, Alkaline-Earth-Metal Cations, and Copper(II). *Inorg. Chem.* **1987**, *26* (16), 2699−2706.
(65) Bailey, G. A.; Price, E. W.; Zeglis, B. M.; Ferreira, C. L.; Boros, E.; Lacasse, M. J.; Patrick, B. O.; Lewis, J. S.; Adam, M. J.; Orvig, C. H2azapa: A Versatile Acyclic Multifunctional Chelator for ^{67}Ga, ^{64}Cu, ^{111}In, and ^{177}Lu. *Inorg. Chem.* **2012**, *51* (22), 12575−12589.
(66) Gottlieb, H. E.; Kotlyar, V.; Nudelman, A. NMR Chemical Shifts of Common Laboratory Solvents as Trace Impurities. *J. Org. Chem.* **1997**, *62* (21), 7512−7515.
(67) Mikkelsen, K.; Nielsen, S. O. Acidity Measurements with the Glass Electrode in H_2O-D_2O Mixtures. *J. Phys. Chem.* **1960**, *64* (5), 632−637.
(68) Patiny, L.; Borel, A. ChemCalc: A Building Block for Tomorrow's Chemical Infrastructure. *J. Chem. Inf. Model.* **2013**, *53* (5), 1223−1228.
(69) Altomare, A.; Burla, M. C.; Camalli, M.; Cascarano, G. L.; Giacovazzo, C.; Guagliardi, A.; Moliterni, A. G. G.; Polidori, G.; Spagna, R. SIR97: A New Tool for Crystal Structure Determination and Refinement. *J. Appl. Crystallogr.* **1999**, *32*, 115−119.
(70) Sheldrick, G. M. A Short History of SHELX. *Acta Crystallogr., Sect. A: Found. Crystallogr.* **2008**, *64*, 112−122.
(71) Farrugia, L. J. WinGX Suite for Small-Molecule Single-Crystal Crystallography. *J. Appl. Crystallogr.* **1999**, *32*, 837−839.
(72) Legdali, T.; Roux, A.; Platas-Iglesias, C.; Camerel, F.; Nonat, A. M.; Charbonnière, L. J. Substitution-Assisted Stereochemical Control of Bispidone-Based Ligands. *J. Org. Chem.* **2012**, *77* (24), 11167−11176.
(73) Szczepaniak, W.; Kuczynski, K. New Preparative Method for Aminomethylphosphonic, Aminoisopropylphosphonic and Iminobis-(Methylenephosphonic) Acids. *Phosphorus Sulfur Relat. Elem.* **1979**, *7*, 333−337.
(74) *Méthodes d'analyse Complexométriques Avec Les Titriplex*; Merck: Darmstadt, Germany, 1990.
(75) Raymond, K. Tragic Consequence with Acetonitrile Adduct. *Chem. Eng. News* **1983**, *61* (49), 4−4.
(76) Gans, P.; O'Sullivan, B. *GLEE*; Protonic Softwares, Leeds, U.K., and Berkeley, CA, 2005.
(77) Gans, P.; O'Sullivan, B. GLEE, a New Computer Program for Glass Electrode Calibration. *Talanta* **2000**, *51* (1), 33−37.
(78) Gans, P.; Sabatini, A.; Vacca, A. Investigation of Equilibria in Solution. Determination of Equilibrium Constants with the HYPERQUAD Suite of Programs. *Talanta* **1996**, *43* (10), 1739−1753.
(79) Alderighi, L.; Gans, P.; Ienco, A.; Peters, D.; Sabatini, A.; Vacca, A. Hyperquad Simulation and Speciation (HySS): A Utility Program for the Investigation of Equilibria Involving Soluble and Partially Soluble Species. *Coord. Chem. Rev.* **1999**, *184*, 311−318.
(80) Gampp, H.; Maeder, M.; Meyer, C.; Zuberbuhler, A. Calculation of Equilibrium-Constants from Multiwavelength Spectroscopic Data 0.1. Mathematical Considerations. *Talanta* **1985**, *32* (2), 95−101.
(81) Alliot, C.; Michel, N.; Bonraisin, A.-C.; Bossé, V.; Laizé, J.; Bourdeau, C.; Mokili, B. M.; Haddad, F. One Step Purification Process for No-Carrier-Added ^{64}Cu Produced Using Enriched Nickel Target. *Radiochim. Acta* **2011**, *99*, 627−630.
(82) Bleiholder, C.; Börzel, H.; Comba, P.; Ferrari, R.; Heydt, M.; Kerscher, M.; Kuwata, S.; Laurenczy, G.; Lawrance, G. A.; Lienke, A.; Martin, B.; Merz, M.; Nuber, B.; Pritzkow, H. Coordination Chemistry of a New Rigid, Hexadentate Bispidine-Based Bis(Amine)Tetrakis-(Pyridine) Ligand. *Inorg. Chem.* **2005**, *44* (22), 8145−8155.
(83) Comba, P.; Grimm, L.; Orvig, C.; Rück, K.; Wadepohl, H. Synthesis and Coordination Chemistry of Hexadentate Picolinic Acid Based Bispidine Ligands. *Inorg. Chem.* **2016**, *55* (24), 12531−12543.
(84) Meyer, M.; Frémond, L.; Tabard, A.; Espinosa, E.; Vollmer, G. Y.; Guilard, R.; Dory, Y. Synthesis, Characterization and X-Ray Crystal Structures of Cyclam Derivatives. Part VI. Proton Binding Studies of a Pyridine-Strapped 5,12-Dioxocyclam Based Macrobicycle. *New J. Chem.* **2005**, *29* (1), 99−108.
(85) Gans, P.; Sabatini, A.; Vacca, A. *HYPERQUAD2000*; Protonic Software, Leeds, U.K., and University of Florence, Florence, Italy, 2000.
(86) Siener, T.; Cambareri, A.; Kuhl, U.; Englberger, W.; Haurand, M.; Kögel, B.; Holzgrabe, U. Synthesis and Opioid Receptor Affinity of a Series of 2, 4-Diaryl-Substituted 3,7-Diazabicylononanones. *J. Med. Chem.* **2000**, *43* (20), 3746−3751.
(87) Kuhl, U.; Englberger, W.; Haurand, M.; Holzgrabe, U. Diazabicyclo[3.3.1]Nonanone-Type Ligands for the Opioid Receptors. *Arch. Pharm.* **2000**, *333*, 226−230.
(88) Hosken, G. D.; Hancock, R. D. Very Strong and Selective Complexation of Small Metal Lons by a Highly Preorganised Open-Chain Bispidine-Based Ligand. *J. Chem. Soc., Chem. Commun.* **1994**, 1363−1364.
(89) Lomozik, L. *Monatsh. Chem.* **1984**, *115*, 261−270.
(90) Hathaway, B. J.; Billing, D. E. The Electronic Properties and Stereochemistry of Mono-Nuclear Complexes of the Copper(II) Ion. *Coord. Chem. Rev.* **1970**, *5* (2), 143−207.
(91) Patel, R. N.; Shrivastava, R. P.; Singh, N.; Kumar, S.; Pandeya, K. B. Equilibrium Studies on Mixed-Ligand Mixed-Metal Complexes of Copper(II), Nickel(II) and Zinc(II) with Glycylvaline and Imidazole. *Indian J. Chem.* **2001**, 361−367.
(92) Clark, W. M. Oxidation-Reduction Potentials of Organic Systems. In *Encyclopedia of Electrochemistry of the Elements*; Marcel Dekker: New York, 1976.
(93) Krebs, H. A.; Kornberg, H. L.; Burton, K. *Energy Transformations in Living Matter: A Survey*; Springer: Berlin, 1957.
(94) Lima, L. M. P.; Halime, Z.; Marion, R.; Camus, N.; Delgado, R.; Platas-Iglesias, C.; Tripier, R. Monopicolinate Cross-Bridged Cyclam Combining Very Fast Complexation with Very High Stability and Inertness of Its Copper(II) Complex. *Inorg. Chem.* **2014**, *53* (10), 5269−5279.
(95) Woodin, K. S.; Heroux, K. J.; Boswell, C. A.; Wong, E. H.; Weisman, G. R.; Niu, W.; Tomellini, S. A.; Anderson, C. J.; Zakharov, L. N.; Rheingold, A. L. Kinetic Inertness and Electrochemical Behavior of Copper(II) Tetraazamacrocyclic Complexes: Possible Implications for in Vivo Stability. *Eur. J. Inorg. Chem.* **2005**, *2005* (23), 4829−4833.
(96) Odendaal, A. Y.; Fiamengo, A. L.; Ferdani, R.; Wadas, T. J.; Hill, D. C.; Peng, Y.; Heroux, K. J.; Golen, J. A.; Rheingold, A. L.; Anderson, C. J.; Weisman, G. R.; Wong, E. H. Isomeric Trimethylene and Ethylene Pendant-Armed Cross-Bridged Tetraazamacrocycles and

DOI: 10.1021/acs.inorgchem.7b01731
Inorg. Chem. XXXX, XXX, XXX−XXX

in Vitro/in Vivo Comparisions of Their Copper(II) Complexes. *Inorg. Chem.* **2011**, *50* (7), 3078−3086.

DOI: 10.1021/acs.inorgchem.7b01731
Inorg. Chem. XXXX, XXX, XXX−XXX